Response to Reviewers

We are grateful to the reviewers for several constructive comments and suggestions that have helped us improve our manuscript. Reviewers' comments are given in red and our response follows in black.

Response to Reviewer 1

1. Comparison between the simulated ice number and observed ice number should be included in the study since this is the aim of this study. If the observation data for ice number is not available for this case, the author should use a different case that has this useful observation data. Otherwise, it is hard to justify if the modification in the model leading in the right direction. Lacking this comparison makes the paper less convincing to readers.

Unfortunately measurements of cloud particle number concentrations were not measured during ASCOS. Such measurements have been collected during Arctic flight campaigns, but these are generally conducted at lower latitudes (e.g. ACCACIA, M-PACE, RACEPAC). Investigations focusing on lower-latitude clouds have been performed (e.g. Sotiropoulou et al. 2020) and indicated a possibly critical role of the examined process. However understanding microphysical interactions over the high Arctic and over multi-year ice-pack is particularly important and that is why ASCOS data (collected at ~87^{o}N) have extensively been used for microphysical investigations and model intercomparisons (e.g. Lowe et al 2017; Stevens et al. 2018; Christiansen et al. 2020), even though there are no detailed microphysical measurements. Thanks to previous studies, a good understanding of how different treatments of ice nucleation and CCN activation impact cloud macrophysical properties has already been established. Here we aim to build on existing knowledge and further quantify the possible impact of SIP. Furthermore, the results can be compared to previous investigations of this process, which also used macrophysical quantities to evaluate the performance of their parameterizations due to a lack of ICNC measurements (e.g. Fridlind et al. 2007; Fu et al. 2019).

2. The scientific contribution is not significant enough for this paper. The implementation of the secondary ice production processes to the model is clearly shown in your previous paper. Just several sensitivities tests are not enough to support a whole research story. More deep analysis should be conducted, like give a physically-based explanation of changes in LWP and IWP, not only just describe the figures feature.

Note that this is the first attempt to describe the process interactively in MIMICA (a parcel-model based parameterization was applied in the previous study). We believe that this work will be useful as a guide for how these processes can and should be considered in global models. Nevertheless, thank you for this comment, as it made us look into the feedbacks between ice multiplication, precipitation, changes in size distributions and sublimation in the subcloud layer more carefully. These parameters are now shown in Figures 4 and 5.

3. The "spectral representation" in the title and "Sensitivity to the representation of the ice particle spectrum" in Page 12 (Line 401) are confused to readers. The representation of the ice particle spectrum indicates the size distribution function, just as the authors described in the paper Line 153 "size distributions are defined by generalized Gamma functions". I think the author did a sensitivity test about the threshold value in the cloud ice and snow autoconversion process, not about the size distribution function. I suggest modifying the title and the subtitle.

The new title is: 'Ice multiplication from ice-ice collisions in the high Arctic: sensitivity to ice habit, rimed fraction, ice type and uncertainties in the numerical description of the process'. This also refers to the new sensitivity tests that concern uncertain parameters of the break-up description, whose conduction was suggested by Reviewer 3.

Minor comments:

1. Page 3 (Line 100) what is the uncertainty range of the instrument and the observation data?

The uncertainty in LWP and IWP, i.e. the macrophysical quantities used to evaluate the results, is already stated in Section 2. We further added uncertainties in radiosonde measurements and CCN measurements, which were used to initialize the simulations. Finally, we now also state the vertical resolution for radar measurements, which indicates the uncertainty in defining cloud boundaries (cloud top and base height).

2. Page 10 (Line 325) "Planar ice is expected to generate more fragments per collision compared to plates if the diameter of the particles and the collisional kinetic energy are the same (see equations 6-7 in Appendix B). " you mean "dendrites ice is expected to generate more fragments per collision compared to plates"?

We apologize, this statement is wrong and has been removed. The same diameter does not imply same collisional kinetic energy, as terminal velocities are differently parameterized for the two ice habits.

3. Page 10 (Line 309) "while the ICNC enhancement from break-up is shown in the Supplementary Information (Text S2, Fig. S2)" I think a X-Y Figure (similar as Figure 2) shows the total ice enhancement is quite important, this figure show be shown in the main text. I also suggest adding a figure shows the comparison between the observed ice number and simulated ice number concentration.

Following the reviewer's suggestion we now have included a figure that shows the mean ICNC and IWP enhancement in the main text (and removed the corresponding figures from SI). Unfortunately there are no observations of ice number concentrations as discussed above.

4. Page 10 (Line 330) "This variability indicates that precipitation processes (i.e.

the precipitation sink) are more effective". Author indicated that the decrease of cloud ice in Figure 3b is due to precipitation sink, but why the graupel number still increase in Figure 3d? considering the graupel has a larger fall speed parameter, should precipitate more quickly compared with cloud ice.

Thank you for spotting this, this statement was indeed wrong. Increases in cloud ice number concentration result in more cloud ice-drop collisions (thus graupel formation) and cloud ice aggregation (thus snow formation). This means that any *Ni* decrease that follows a *Ni* enhancement is due to cloud-ice depletion through snow and graupel formation (not through precipitation). This is why fluctuations in *Ni* correlate with fluctuations in *Ng* and *Ns* in Figure S2 (which corresponds to the old Figure 3 in the previous manuscript). Due to a larger number of figures being included in the main text to study the influence of precipitation, sublimation and particle size, we have moved this figure to the supplementary information.

5. Page 32 (Line 1000) In Table 1, the parameters av for graupel is set to be 199.05 in the model, However, the av is usually set to be 19.3 for graupel, and is 114 for hail (Morrison et al, 2009). So, 200 seems too large for me, is any citation here to support that the Arctic graupel has big value av?

In Milbrandt and Morrison (2013), the a_v parameter is set to 62.92 for graupel particles with a density of 50 kg m^{-3} (see Table 2 in their study) and 189.02 for a density of 850 kg m^{-3}. However in many other microphysics schemes a substantially lower a_v is assumed. We could not find terminal velocity parameters specifically constrained for Arctic graupel in the literature, but since convective motions in the Arctic are weak it does make more sense to adapt the lower values.

Following the reviewer's suggestion, snow and graupel parameters in the mass-diameter and fallspeed-relationships have been replaced with those from the Morrison scheme in the revised study. While this has a negligible effect on the CNTRL simulation, it has a greater effect on ice multiplication, since fragment generation is a function of collisional kinetic energy. For moderate ice production the effect was weak. For example in BRDEN0.2 the maximum total fragment generation rate was 1.4 L^{-1}s^{-1} while now it does not exceed 1.1 L^{-1}s^{-1}. In BRPLA0.4 however, where explosive multiplication occurs, the maximum fragment generation rate was 73.6 L^{-1}s^{-1} in the old simulation setup while now it has decreased to 12.84 L^{-1}s^{-1}. An important impact was also found in simulations with active cloud ice-to-snow autoconversion. Enhancing snow formation results in enhanced ice multiplication; however if large terminal velocity parameters are used, the enhancement can be significantly larger. This is why adapting a low separation diameter (125 μm) for cloud ice and snow resulted in substantially more multiplication than when adapting the 500-μm threshold and thus limiting break-up of snow; note that snow-graupel collisions are the main source of fragments. In the new simulations with more moderate terminal velocities, enhancement of break-up through autoconversion results in moderate increases in fragment generation. For this reason the sensitivity of our results to the choice of the cloud ice-to-snow critical diameter has substantially decreased. This is now stated in lines 329-330, while only results for the 500-μm threshold are shown in the relevant figures.

6. Page 36 (Line 1070) In Figure 2, does this mean observed LWP and IWP does not change during this time period? This figure is kind of confused, I suggested use time-series of observed LWP and IWP with uncertainty.

Note that the Large Eddy Simulation does not account for changes in the large-scale forcing and aerosol conditions and thus eventually develops a cloud in a quasi-equilibrium state. In reality the 'steady' stratocumulus cloud lasted only for about twelve hours, while aerosol conditions likely changed substantially after this (Stevens et al. 2018). And even within these 12 hours vertical displacements associated with changes in the vertical large-scale forcing were observed, which cannot be captured by any LES model (see Figure 11 in Stevens et al 2011). Moreover, the model requires a relatively long spin-up time to develop its physics, so observation-model comparisons at each timestep are not very consistent. Thus LES simulations are in a sense semi-idealized. For all these reasons we use the macrophysical statistics from the 'steady' cloud layer period to evaluate our simulations (this is explained in lines 150-155). Point observations are, however, presented in the study in the RFD plots (Figures 9-10) to evaluate phase-partitioning in the model.

7. Page 36 (Line 1070) From Figure 2, the simulated LWP decreased by 50 g m^{-2}, but IWP only increased by 5 g m^{-2}. Does this means the total condensation is decreased? Or precipitation is increased?

Both precipitation and sublimation in the sub-cloud layer increased. The feedbacks between ice multiplication and these processes are now discussed more extensively in the revised text (Section 4.1 / Figure 4).

8. Page 37 (Line 1095) Figure 3e does not have a black line, does this mean control simulation do not has snow?

Yes, snow number concentrations do not exceed threshold values (10^{-4} L^{-1}) in the CNTRL simulation. This is because snow is only treated as aggregate in the default MIMICA version and cloud ice–cloud ice collisions are not favored in the CNTRLDEN simulation. Once break-up is activated, multiplication of cloud ice results in more collisions between these particles and promotes snow formation. This is discussed in lines 372-377 in the revised text.

9. Page 37 (Line 1095) Figure 3 shows graupel is the dominant ice-phase particles, it is 2 orders of cloud ice and is 3-4 orders of snow. Is that true for Arctic cloud? Graupel is the dominant ice particles in the Arctic cloud? Or it is a model dependent result? I think snow and cloud ice should have the largest fraction of total ice.

Graupel can be dominant in some cases in Arctic clouds (e.g. Fitch et al. 2020), although graupel formation has been linked to the existence of convective cells in the past (Lawson and Zuidema 2009). A recent study however suggests that static destabilization through cloud-top radiative cooling can favor graupel formation in Arctic boundary-layer clouds. Nevertheless, for the examined case graupel formation is indeed a model-dependent result. Polarimetric radar measurements are not available to evaluate this behaviour. In the ASCOS intercomparison project (Stevens et al., 2018), where five models with bulk ice microphysics were compared, COSMO-LES produced only cloud ice. WRF simulated only snow, while COSMO-NWP and UM-CASIM resulted in both snow and little cloud ice, with snow being very little in the former. Note that all these models were constrained with the same primary ice production rate. MIMICA was the only model that produced graupel, however it was among the models (including UM-CASIM) that resulted in more realistic IWC values (see Figure 11 in Stevens et al. 2018), while all other models predicted very little ice content. The fact that ice type is model-dependent and the reason why MIMICA promotes riming compared to other models is now discussed extensively in lines 303-314.

Response to Reviewer 3

We are grateful to the reviewer for several constructive comments and suggestions that have helped us improve our manuscript. The reviewer's comments are given in red and our response follows in black.

Major Comments

The results are impressive with greatly improved agreement to observations when breakup in ice-ice collisions is included. This vindicates the vision of Schwarzenboek *et al*. (2009) who made observations of this breakup occurring in Arctic clouds. It would be nice to compare the current prediction with their observations. If they measured that roughly half of all ice crystals had branches missing, is this consistent with the ice enhancement ratio of 2 measured ? Likewise with Rangno and Hobbs (2001).

We thank the reviewer for his/her comments. Rangno et al. found that about 35% of the observed ice particles have likely been produced by ice-ice collisions. This is generally consistent with the 1.5-2fold enhancement of ICNCs found in our simulations. Schwarzenboek et al. (2009) found an indication of fragmentation in 55% of their samples; however, they could confirm natural fragmentation only for 18%. The fragments generated per collision were estimated to be typically less than 5 in their study (with 1-branch crystals being more frequent). Our model predicts that only 10-12% of the particles contribute to fragmentation but a larger number of fragments (of the order of ~10) is generated per snow-graupel collision. However, Schwarzenboek et al. examined particles with sizes about 300 μm or somewhat larger. In our study, mm-size particles dominate ice multiplication. Thus, generation of more fragments per collision is expected.

A discussion on the ice particle sizes that contribute to multiplication is added in section 4.1. A qualitative comparison of the ICNC enhancement factors found in our simulations and in the results in Rangno and Hobbs (2001) is also offered in the same section, lines 421-424. Differences between our findings and Schwarzenboek et al. (2009) results are discussed in the 'Discussion' section.

There is some uncertainty in the breakup treatment. As a sensitivity test, it might be

worth removing the correction factor (to correct for sublimational weakening in Vardiman's data) in the breakup scheme by Phillips et al. (2017a): what is the effect from such uncertainty ? Alternatively, if the number of fragments per collision is altered within the range of uncertainty apparent from the error-bars (a factor of 3 uncertainty) in the plots by Phillips et al., does this drastically affect the cloud simulation ?
We added sensitivity tests in which the sublimation correction factor has been removed from the parameterization. This resulted in explosive multiplication and cloud glaciation for both simulations with dendrites and plates. Activating ice-to-snow autoconversion, and thus enhancing precipitation, prevents cloud glaciation in simulations with dendrites but not for plates. These results are discussed in section 3.3.4

It would be good to include a short model description perhaps near Section 3. After reading the paper, I am still unclear if MIMICA is bin or bulk microphysics and what its microphysical species are. It seems to be bulk microphysics only.
MIMICA includes a bulk microphysics scheme, this is now explicitly stated in Section 3.1 to avoid confusion. Also, a summary of all the included ice-liquid interactions is now given in the same section, while the corresponding formulas can be found in Wang and Chang (1993).

One wonders if sublimational breakup will further improve agreement with the observations when it is treated in models. If sublimation is happening in the cloud, then this might boost the breakup in ice-ice collisions by weakening the ice.
Examination of the domain-averaged profiles of saturation with respect to ice does not indicate subsaturated conditions within the cloud. This is now mentioned in the 'conclusions' section.

It would be good to apply the theory by Yano and Phillips (2011) to understand why the ice multiplication is weak in these Arctic clouds. You can estimate first the order of magnitude of the time for growth of snow particles to become graupel, given the typical LWC. If one replaces the "small graupel" in the theory by Yano and Phillips by "snow", then that time-scale (tau_g) gives the order of magnitude of the multiplication efficiency (c_tilde) measuring the instability of the system of ice multiplication. The average number of fragments per graupel-snow collision would be needed too. Phillips et al. (2017b) did such estimates for their multicell convective system to estimate c_tilde and so it should be possible to do here. The authors will probably find, if they do this theoretical estimate, that the Arctic clouds are weakly unstable because the LWC is weak.
We derived tau_g from two simulations, which was found to be shorter than in previous studies (7-8 min). For BRDEN0.2 and BRPLA0.2 we estimated $\hat{C}$=1.6 and $\hat{C}$=2.2 respectively. Indeed while $\hat{C}>1$, which indicates that explosive multiplication is possible, these values are substantially smaller than the value $\hat{C}$=10 estimated for a convective cloud by Phillips et al. (2017b) and for warmer Arctic clouds by Sotiropoulou et al. (2020). This is now discussed in the 'Discussion' section.

Detailed comments
Abstract
I am not sure if it is entirely accurate to say that habit and rimed fraction are "poorly constrained". Habit is something observe-able in the aircraft data (e.g. observations of

axial ratio of ice particles from aircraft flights are sometimes used for model validation). Perhaps what is meant here is that most models do not have the detail required to predict these explicitly. Some models do have the detail (e.g. Hebrew University Cloud Model, which has a bin microphysics scheme with dendrites, columns etc as separate species and rimed fraction).
Since a dendrite is a type of planar particle (axial ratio < 1), it might be more accurate to describe these two habits as "non-dendritic planar" particles and "dendrites".
Thank you for this clarification. This statement has been removed from this section. We now simply discuss the fact that while most bulk microphysics schemes do not predict ice habit and rimed fraction, according to our results this is not detrimental for the representation of ice multiplication due to break-up. This is particularly important for climate models, which often employ more simplified bulk schemes (e.g. Morrison and Gettelman 2009). Finally, the term 'planar' has been replaced with 'non-dendritic planar' throughout the text.

1. Introduction

Line 56: There is a missing reference: Fu et al. is cited but not listed.
The reference has now been added

Line 59: The paper by Schwarzenboek *et al*. (2009) is by far the most important work underpinning the present study. So it needs more detail in description of how they observed breakup in the Arctic. Need to describe how they distinguished between artificial breakup on impact with the aircraft and natural breakup in the cloud before sampling.
We added a paragraph in the introduction that describes the results of this study: *'Schwarzenboeck et al. (2009) found evidence of crystal fragmentation in 55% of their in-situ samples of ice particles collected with a Cloud Particle Imager during ASTAR (Arctic Study of Aerosols, Clouds and Radiation) campaign. However, natural fragmentation could only be confirmed for 18% these cases, which was identified by either subsequent growth near the break area or/and lack of a fresh break-up line (which indicates shattering on the probe). For the rest of their samples, artificial fragmentation could not be excluded. Moreover, their analysis included only crystals with stellar shape and sizes around 300 μm or roughly larger. This suggests that the frequency of collisional break-up in Arctic clouds is likely higher in reality compared to what is indicated in their study'*

Line 69: Where it is written "*Both studies, however, focused on relatively warm polar clouds (-3^{o}C to -8^{o}C), where rime-splintering is also active*", the impression is conveyed that the H-M process is comparable to the ice-ice collisional breakup. But when one reads the papers cited one sees it was only weakly active. Clarify.
It is now clarified that rime-splintering was weak in both studies. However, in Sotiropoulou et al. (2020) the combination of both rime-splintering and collisional break-up was essential to explain observed ICNCs, while in Sotiropoulou et al. (2021) rime-splintering had hardly any impact.

Lines 56 and 57: Both lab/field studies by Vardiman and Takahashi et al. underpinned the Phillips et al. scheme and both involved some uncertainties. It would be a good idea to mention key issues with their experiments. For example:
· _First, the particles sampled by Vardiman were on a mountainside, apparently below cloud-base, and so there was likely some sublimation before impact, which may be have weakened them. Phillips et al. (2017) had to correct for this, by adjusting the

fragility coefficient inside the exponential function of the scheme. It is a large correction.

· _Second, Takahashi et al. did not observe collisions between two riming particles, but rather observed a riming ice sphere colliding with an ice sphere predominantly in vapour growth (not riming). Thus, there are issues of representativeness. However, in real clouds, graupel falls in and out of zones rich in liquid, so the Takahashi-type collisions between graupel may be representative in a sense in view of the nonlinearity of ice multiplication.

· _Third, we do not have observations of columns or needles breaking up, so the Phillips scheme just treats them as if they are (non-dendritic) planars. It is not ideal.

Thank you for all these points! These key problems regarding the Vardiman and Takahashi et al. studies are now discussed in detail in the Introduction section. The simplification regarding the treatment of column and needles as planar ice is also explicitly stated now.

Despite such biases, Yano and Phillips (2011) argue that errors in the breakup rate per particle actually are not so important, because an explosion of ice concentration occurs anyway provided a threshold is surpassed. In future work, one hopes that MIMICA can predict rimed fraction somehow. It might be more accurate to say something to the effect that these quantities are not explicitly predicted by most cloud models currently.

The explicit treatment of rimed fraction is planned as the subject of future studies. However, the general low sensitivity of our results to rimed fraction (as long as sufficient snow formation is allowed) is very encouraging regarding the representation of this process in less detailed bulk microphysics schemes. This is now discussed in the 'Discussion' and 'Conclusions' section. However we acknowledge that the explicit prediction of rimed fraction is likely critical in conditions characterized by larger multiplication efficiency of the break-up process.

Line 71: The simulated range of in-cloud temperatures is stated. But it is more important to know the actual cloud-top temperature of the cases. So we are now simulating clouds with tops in the dendritic regime where we expect more fragmentation?

This statement is now modified to indicate the cloud-top temperature range: -9.5^{o}C to -12.5^{o}C. Both plates and dendrites can form in this range. -12^{o}C is used as threshold in Phillips et al. (2017a) to separate the temperature ranges that likely favor non-dendritic or dendritic ice habits (with planar shapes being somewhat more likely).

4. Results

4.1 Sensitivity to ice habit

Line 288: There may be a typo or error here: "*Planar ice is expected to generate more fragments per collision compared to plates if the diameter of the particles and the collisional kinetic energy are the same (see equations 6-7 …*". Those two equations are for non-dendritic planars and dendrites respectively. A plate is a special type of (non-dendritic) planar. In this section, it needs to be mentioned that the non-dendritic planars occupy a wider range of temperatures than the dendrites (if this is so here), which boosts the impact from non-dendritic planars.

Thank you, the statement was indeed wrong and has been removed. In MIMICA the characteristic parameters in mass and terminal velocity relationships remain constant throughout the simulation. This means that the ice habit remains constant and does not change as a function of temperature. However the examined temperature range is generally limited anyway as mentioned in our previous reply to a comment above.

4.2 Sensitivity to rimed fraction

Line 358: Why is cloud-ice supposed to have as high a rime fraction as snow ? Riming does not start until sizes of a few hundred microns typically (PK97). Need to denote the size range of "cloud-ice" here.

Indeed this is a simplification. However snow is treated as aggregate in the default MIMICA version, which means that cloud-ice can freely grow to large sizes without necessarily being converted to snow (since cloud ice-to-snow autoconversion is not treated). Offline estimates of the mean particle diameter indicated two modes in the relative frequency distribution of this parameter (Figure 1). The first one indicates small cloud particles ~200-250 μm and the second one mm-particles (found in the lower portion of the cloud). The fact that an increase in rimed fraction only affect the second mode of the distribution suggests that it is the mm-particles that contribute to collisional break-up. This mode has a comparable size to the snow category, thus the simplification of assuming the same rimed fraction for both ice types is not unreasonable. This is now discussed in section 4.1 (note we have now merged the subsections that concern ice habit and rimed fraction).

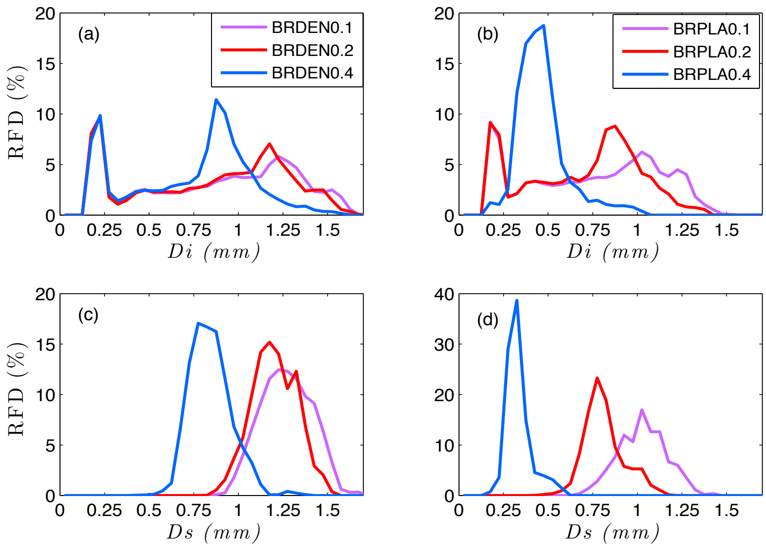

Figure 1: Relative frequency distrubtion of the mean (a, b) cloud ice and (c, d) snow diameter for simulations with (a,c) dendrites and (b, d) plates. Purple, red and blue lines correspond to a prescribed rimed fraction of 0.1, 0.2 and 0.4 for the cloud ice and snow particles than undergo break-up.

4.3 Sensitivity to autoconversion

What is the difference in microphysical processes that cloud-ice and snow are participating in? This seems to be the reason for the sensitivity of this size threshold. I think the best treatment of this autoconversion is from Ferrier (1992) as it preserves the slope parameter when converting cloud-ice to snow.

A summary of the interactions between liquid and ice particles is now offered in section 3.1. However we did find the reason behind the large sensitivity of the multiplication efficiency to the size threshold adapted for cloud-ice-to-snow autoconversion. As pointed out by reviewer 1, the characteristic parameters used for the graupel terminal velocity in the default MIMICA version are large (about one order of magnitude larger than in other stratocumulus schemes). Decreasing the a_v parameter by a factor of ~10 (adapted from Morrison et al. 2005) has a negligible impact on simulations that do not account for collisional break-up. However, since collisional kinetic energy impacts the multiplication efficiency, these changes have a substantial impact on simulations with active break-up. In BRDEN0.2 the maximum total fragment generation rate was 1.4 $L^{-1}s^{-1}$ while now it does not exceed 1.1 $L^{-1}s^{-1}$. In BRPLA0.4, where explosive multiplication occurs, the sensitivity of fragment generation rate is even larger: a maximum rate of 73.6 $L^{-1}s^{-1}$ was found in the old simulation, while now it has decreased to 12.84 $L^{-1}s^{-1}$. A notable impact was also found in simulations with active cloud ice-to-snow autoconversion. Enhancing snow formation results in enhanced ice multiplication; however if large terminal velocity parameters are adapted, the enhancement can be significantly larger. This is why a low separation diameter (125 μm) for cloud ice and snow resulted in more multiplication than when adapting the 500-μm threshold and thus limiting break-up of snow; note that snow-graupel collisions are a main source of fragments (Figure 3). In the new simulations with more moderate terminal velocities, enhancement of break-up through autoconversion results in moderate increases in fragment generation. For this reason the sensitivity of our results to the choice of the cloud ice-to-snow critical diameter has substantially decreased. This is now stated in lines 321-322, while only results for the 500-μm threshold are shown in the relevant figures (note that autoconversion results are discussed in section 4.2 in the revised manuscript).

To conserve the highest moments of the ice particle spectrum, Ferrier et al. (1994) assumes that the number of cloud ice are approximately constant by converting only a few large ice crystals into snow. Thus snow formation does not prevent the accumulation of ice crystals within the cloud layer (since these are not depleted through the autoconversion process) and consequently does not prevent excessive multiplication and cloud glaciation. The simulations with the Ferrier scheme are not shown since they are similar to the runs without autoconversion; however the results are now discussed in section 4.2.

5. Discussion

Line 458: The rimed fraction noted in this sentence does not seem so low in actuality: *"Uncertainties in ice habit are in general not important as long as a low rimed fraction (~0.2) is assumed*". The Phillips et al. (2017a) scheme recommends a default value of 0.1 for the rimed fraction for snow > 1 mm being linearly interpolated to zero at sizes of 0.1 mm (cloud-ice). They actually simulated the rime fraction in their models and 0.1 was more or less what was predicted for a cold cloud-base.

Note that riming is treated differently among models. This is the reason why substantial differences in the distribution of cloud ice content among the different ice types is found for different models (Stevens et al. 2018). This is now discussed in section 3.3.3. MIMICA allows graupel to form from cloud ice particles as small as 150 μm, while accretion efficiency increases with size. Nevertheless, we added simulations with a prescribed rimed fraction of 0.1; the results are very similar to the simulations with $\Psi=0.2$.

Could there be some compensation of errors among different parts of the microphysics? It is possible that, although MIMICA now appears to be a fine model, the current state of knowledge in laboratory observations of ice microphysics is still

limited. Any model is only as good as the empirical basis underpinning it.
Compensation errors are common in models, so this is possible. This can be particularly true for bulk microphysics schemes, where non-physical thresholds are used to separate cloud ice, snow and graupel particles; these thresholds are often tuned differently among different schemes. However this is something that cannot be inferred from our simulation results.

Need to mention possibility of other overlooked SIP processes also playing a role in Arctic clouds. See Field *et al.* (2017). For example, sublimational breakup might be important for Arctic clouds, since downdrafts only need to descend by a few hundred meters to go from being water saturated to ice saturated if adiabatic with constant vapour mixing ratio. There are other ideas, such as the notion of enhanced supersaturations in the wake of falling precipitation particles, which was mentioned at AGU this year.
We added a paragraph regarding the potential influence of sublimation break-up and blowing snow in the discussion section:

'Moreover, while processes like rime-splintering and drop-shattering are clearly ineffective in the examined conditions, the contribution from other SIP mechanisms has not been investigated, e.g. blowing snow and fragmentation of sublimating particles (Field et al. 2017). Sublimation of cloud ice particles can occur if cloud conditions become subsaturated with respect to ice; however a preliminary inspection of the domain-averaged supersaturation profiles did not reveal any such evidence. Furthermore, blowing snow is associated with relatively high wind speeds (Gossart et al, 2017), while during the examined ASCOS case the maximum wind speed never exceeded 5.2 m s^{-2} in the boundary layer.'

Unfortunately, currently we have no consensus about the possibility of activation of additional INPs in transient supersaturations in real cloud conditions

Do the present results accord with aircraft observations by Schwarzenboek et al. who published a histogram of missing branches per particle in Arctic clouds ?
Schwarzenboek et al. (2019) examined ice particles with sizes around 300 μm or somewhat larger and found that a maximum of ~5 fragments are generated per collision. However, they emphasize in their study that the findings are representative only for the specific flight conditions and cannot be generalized for any other ASTAR flights. Thus it is even more unlikely that these results are representative for ASCOS. In our simulations up to 13 fragments can be generated upon snow-graupel collisions, which is substantially larger than the findings in Schwarzenboek et al. (2019). However given that snow particles in MIMICA reach mm-sizes (Fig. 5), model estimations are not unreasonable. A related discussion has been added in the 'Discussion' section on lines 547-550, although no direct comparison between ASCOS simulations and ASTAR data can be conducted.

6. Conclusions
Line 535: Rimed fraction is noted as a poorly constrained yet very sensitive variable for the scheme. A problem here is that it is easy to predict rimed fraction explicitly: you just include a passive scalar for the rime on snow per unit mass of air and then diagnose the rime fraction as a function of size (see Appendix Aa of Phillips et al. 2017b (Part 2)). When will rimed fraction be predicted instead of prescribed in model

development ?

Rimed fraction is not a very sensitive variable; simulations with dendrites give similar results independently of the prescribed rimed fraction. The only set-up that is very sensitive to rimed fraction is BRPLA0.4, thus only if highly rimed plates are assumed. This results in accumulation of many ice crystals in the cloud and eventually glaciation. But if the precipitation sink is enhanced through cloud ice-to-snow autoconversion in this set-up, the rimed fraction does not cause substantial changes in the cloud macrophysical state anymore.

The fact that our results show generally low sensitivity to the prescribed rimed fraction is positive news for larger-scale models, which employ bulk microphysics schemes that do not predict rimed fraction. Even more so, for climate model schemes like Morrison and Gettelman 2009 that do not even account for rimed particles (graupel). However, we acknowledge that this conclusion likely concerns only conditions with weak efficiency of break-up, as those examined here. Rimed fraction is expected to play a more critical role in more convective conditions and its explicit prediction is included in future model development plans. This is now discussed in the 'conclusions' section.

Appendix

When the Phillips scheme is applied, is there a temporary grid of size bins constructed so as to apply the breakup scheme for each colliding bin-pair?

The microphysics scheme already includes bulk descriptions for the interactions between the different ice types and within the same ice category, as aggregation is accounted for in the model. For consistency with the rest of the code, the same relationships are used to describe ice-ice collisions for ice multiplication. Thus a bulk (instead of a bin) approach is used for all processes in the model, including SIP. This is now explicitly stated at the beginning of the Appendix to avoid any confusion.

References:

Christiansen, S., Ickes, L., Bulatovic, I., Leck, C., Murray, B. J., Bertram, A. K., et al.: Influence of Arctic microlayers and algal cultures on sea spray hygroscopicity and the possible implications for mixed-phase clouds. *Journal of Geophysical Research: Atmospheres*, 125, e2020JD032808. https://doi.org/10.1029/2020JD032808, 2020

Fitch, Kyle E; Garrett, Timothy J.Earth and Space Science Open Archive ESSOAr; Washington, Jun 28, 2020.DOI:10.1002/essoar.10503407.1 (submitted to GRL)

Fridlind, A. M., Ackerman, A. S., McFarquhar, G., Zhang, G., Poellot, M. R., DeMott, P. J., Prenni, A. J., and Heymsfield, A. J.: Ice properties of single-layer stratocumulus during the Mixed-Phase Arctic Cloud Experiment: 2. Model results., J. Geophys. Res., 112, D24202, https://doi.org/10.1029/2007JD008646, 2007.

Fu, S., Deng, X., Shupe, M.D., and Huiwen X.: A modelling study of the continuous ice formation in an autumnal Arctic mixed-phase cloud case, Atmos. Res., 228, 77-85, https://doi.org/10.1016/j.atmosres.2019.05.021, 2019

Lawson R. P. & Zuidema P., Aircraft Microphysical and Surface-Based Radar, Observations of Summertime Arctic Clouds, *Journal of the Atmospheric Sciences*, *66 (12), 3505-3529*

Loewe, K., Ekman, A. M. L., Paukert, M., Sedlar, J., Tjernström, M., and Hoose, C.: Modelling micro- and macrophysical contributors to the dissipation of an Arctic mixed-phase cloud during the Arctic Summer Cloud Ocean Study (ASCOS), Atmos. Chem. Phys., 17, 6693–6704, https://doi.org/10.5194/acp-17-6693-2017, 2017.

Stevens, R. G., Loewe, K., Dearden, C., Dimitrelos, A., Possner, A., Eirund, G. K., Raatikainen, T., Hill, A. A., Shipway, B. J., Wilkinson, J., Romakkaniemi, S., Tonttila, J., Laaksonen, A., Korhonen, H., Connolly, P., Lohmann, U., Hoose, C., Ekman, A. M. L., Carslaw, K. S., and Field, P. R.: A model intercomparison of CCN-limited tenuous clouds in the high Arctic, Atmos. Chem. Phys., 18, 11041–11071, https://doi.org/10.5194/acp-18-11041-2018, 2018.

Ice multiplication from ice-ice collisions in the high Arctic: sensitivity to ice habit, rimed fraction, ice type and uncertainties in the numerical description of the process

Georgia Sotiropoulou[1,2], Luisa Ickes[3], Athanasios Nenes[2,4] and Annica M. L. Ekman[1]

[1]Department of Meteorology, Stockholm University & Bolin Center for Climate Research, Stockholm, Sweden

[2]Laboratory of Atmospheric Processes and their Impacts, School of Architecture, Civil & Environmental Engineering, Ecole Polytechnique Fédérale de Lausanne, Lausanne, Switzerland

[3]Department of Space, Earth and Environment, Chalmers University of Technology, Gothenburg, Sweden

[4]Institue for Chemical Engineering Sciences, Foundation for Research and Technology Hellas, Patras, Greece

Correspondence: georgia.sotiropoulou@misu.su.se

Abstract. Atmospheric models often fail to correctly reproduce the microphysical structure of Arctic mixed-phase clouds and underpredict ice water content, even when the simulations are constrained by observed levels of ice nucleating particles. In this study we investigate whether ice multiplication from break-up upon ice-ice collisions, a process missing in most models, can account for the observed cloud ice in a stratocumulus cloud observed during the Arctic Summer Cloud Study campaign. Our results indicate that the efficiency of this process in these conditions is weak; increases in fragment generation are compensated by subsequent enhancement of precipitation and subcloud sublimation. Activation of collisional break-up improves the representation of cloud ice content, but cloud liquid remains overestimated. In most sensitivity simulations, variations in ice habit and prescribed rimed fraction have little effect on the results. A few simulations result in explosive multiplication and cloud glaciation; however, in most set-ups, the overall multiplication effects become substantially weaker if the precipitation sink is enhanced through cloud ice-to-snow autoconversion. The largest uncertainty stems from the correction factor for ice enhancement due to sublimation included in the break-up parameterization; excluding this correction results in rapid glaciation, especially in simulations with plates. Our results indicate that the lack of a detailed treatment of ice habit and rimed fraction in most bulk microphysics schemes is not detrimental for the

Georgia 18/3/2021 13:52
Comment [1]: New text additions are highlighted in yellow

description of collisional break-up process in the examined conditions, as long as cloud ice-to-snow autoconversion is considered.

Introduction

Cloud feedbacks play an important role in Arctic climate change (Cronin and Tziperman, 2015; Kay et al., 2016; Tan and Storelvmo, 2019) and sea-ice formation (Burt et al., 2015; Cao et al., 2017). However, despite their significant climatic impact, Arctic mixed-phase clouds remain a great source of uncertainty in climate models (Stocker et al., 2013; Taylor et al., 2019). To accurately predict the radiative effects of mixed-phase clouds in models, an adequate description of their microphysical structure, such as the amount and distribution of both liquid water and ice, is required (Korolev et al., 2017). Both ice nucleation and liquid drop formation require seed particles to be present known as ice nucleating particles (INPs) and cloud condensation nuclei CCN), respectively. However, the observed ice crystal number concentrations (ICNCs) are often much higher than the observed INP concentrations in the Arctic (Fridlind et al., 2007; 2012; Gayet et al., 2009; Lloyd et al., 2015), where INPs are generally sparse (Wex et al., 2019). Moreover, model simulations constrained by INP measurements frequently underpredict the observed amount of ice (Fridlind and Ackerman, 2019).

Secondary Ice Processes (SIP) have been suggested as the reason why ice crystal concentrations exceed INP levels (Field et al., 2017; Fridlind and Ackerman, 2019). SIP involve the production of new ice crystals in the presence of pre-existing ice, without requiring the presence of an INP. The most well-known mechanism is rime-splintering (Hallet and Mossop, 1974), which refers to the ejection of ice splinters when ice particles collide with supercooled liquid drops. Rime-splintering is active only in a limited temperature range, between -8^{o}C and -3^{o}C, and requires the presence of liquid droplets both smaller than 13 μm and larger than 25 μm (Hallett and Mossop, 1974; Choularton et al., 1980). Moreover, recent studies have shown that rime-splintering alone cannot explain the observed ICNCs in polar clouds even within the optimal temperature range (Young et al., 2019; Sotiropoulou et al., 2020a,b). Ice fragments may also be generated when a relatively large drop freezes and shatters (Lauber et al., 2018; Phillips et al., 2018); drop-shattering, however, has been found insignificant in polar conditions (Fu et al., 2019; Sotiropoulou et al., 2020). Finally, ice multiplication can occur from mechanical break-up due to ice-ice collisions (Vardiman et al., 1978; Takahashi et al., 1995). This process has been also indentified in in-situ measurements of Arctic clouds (Rangno and Hobbs, 2001; Schwarzenboeck et al., 2009).

Schwarzenboeck et al. (2009) found evidence of crystal fragmentation in 55% of in-situ observations of ice particles collected with a Cloud Particle Imager during ASTAR (Arctic Study of Aerosols, Clouds and Radiation) campaign. However, natural fragmentation could only be confirmed for 18% these cases, which was identified by either subsequent growth near the break area or/and lack of a fresh break-up line (which indicates toward shattering on the probe). For the rest of their samples, artificial fragmentation could not be excluded. Moreover, their analysis included only crystals with stellar shape and sizes round 300 μm or roughly larger. This suggests that the frequency of collisional break-up in Arctic clouds is likely higher in reality compared to what is indicated in their study. Yet, despite the potential impact of this process in Arctic conditions, it has received little attention from the modeling community.

Fridlind et al. (2007) and Fu et al. (2019) investigated the contribution from ice-ice collisions in an autumnal cloud case observed during the Mixed-Phase Arctic Cloud Experiment (M-PACE) and found that the process could not account for the observed ice content at in-cloud temperatures between -8.5^{o}C and -15.5^{o}C. The parameterization of the break-up process used in these studies was based on the laboratory data of Vardiman (1978). However, there are significant shortcomings in the available laboratory measurments. For example, in Vardiman (1978) the ice particles were collected in a mountainside below cloud base, thus the collected samples were impacted by sublimation. Takahashi et al. (1995) also used an unrealistic set-up: they performed collisions between cm-size hailballs, while one of the colliding hydrometeors was unrimed and fixed. These considerations preclude deriving an accurate parameterizaton for ice multiplication due to collisional break-up from this data alone.

Phillips et al. (2017a,b) developed a more advanced treatment of ice multiplication from ice-ice collisions, which is based on the above mentioned laboratory results, but further considers the impact of collisional kinetic energy, ice habit, ice type and rimed fraction. More specifically, their parameterization accounts for dendritic and non-dendritic planar ice shapes; the latter includes plates, columns and needles, thus all the ice habits for which there are no available observations of break-up. Moreover, to correct the effect of sublimation in Vardiman's (1978) data, they adjusted the fragile coefficient (term ψ in Appendix A) in their description. While these approximations are a source of uncertainty, their parameterization has been tested in polar clouds (Sotiropoulou et al. 2020; 2021) and resulted in ice enhancements that could explain the observed ICNCs. Sotiropoulou et al. (2020; 2021) focused on relatively warm polar clouds (-3^{o}C to -8^{o}C), for which rime-splintering is considered to be the dominant SIP mechanism; yet the efficiency of this process alone was found to be limited in these studies. In Sotiropoulou et al. (2020) the combination of both rime-splintering and collisional break-up was essential to explain observed ICNCs, while in Sotiropoulou et al. (2021) rime-splintering had hardly any impact.

In this study, we aim to investigate the role of ice-ice collisions at a somewhat colder in-cloud temperature range than in Sotiropoulou et al. (2020) and (2021). The simulated cloud-top range (-9.5°C to –12.5°C) includes temperatures for which previous parameterizations found limited efficiency of the process (Fridlind et al., 2007; Fu et al., 2019). The Phillips parameterization is implemented in the MIT-MISU Cloud-Aerosol (MIMICA) Large Eddy Simulation (LES) model to examine its performance for a stratocumulus case observed during the Arctic Summer Cloud Study (ASCOS) campaign in the high Arctic. To identify the optimal microphysical conditions for ice multiplication through collisional break-up, the sensitivity of the results to the assumed rimed fraction, ice habit and ice type (e.g. cloud ice/ snow) of the colliding ice particles is examined.

2. Field observations

The ASCOS campaign was deployed on the Swedish icebreaker *Oden* between 2 August and 9 September 2008 in the Arctic Ocean, to improve our understanding of the formation and life-cycle of Arctic clouds. It included an extensive suite of in-situ and remote sensing instruments, a description of which can be found in Tjernström et al. (2014). Here we only offer a brief description of the instruments and measurements utilized in the present study.

2.1. Instrumentation

Information on the vertical atmospheric structure was derived from Vaisala radiosondes, released every 6 hours, with 0.15°C and 3% uncertainty in temperature and relative humidity profiles, respectively. Cloud boundaries were derived from a vertically-pointing 35 GHz Doppler Millimeter Cloud Radar (MMCR; Moran et al., 1998) with a vertical resolution of 45 m and two laser ceilometers. CCN concentrations were measured by an in-situ CCN counter (Roberts and Nenes, 2005), set at a constant supersaturation of 0.2% (with an uncertainty of ±0.04%; Moore et al. 2011) based on typical values used in other similar expeditions (Bigg and Leck, 2001; Leck et al., 2002). The total uncertainty in CCN concentration derived from counting statistics and fluctuations in pressure and flow rate is 7–16% for CCN concentrations above 100 cm^{-3} (Moore et al., 2011). Vertically-integrated liquid water path (LWP) was retrieved from a dual-channel microwave radiometer, with an uncertainty of 25 g m^{-2} (Westwater et al., 2001). Ice water content (IWC) was estimated from the radar reflectivity observed by the MMCR, using a power-law relationship (e.g. Shupe et al, 2005), with a factor of 2 uncertainty.The ice water path (IWP) was integrated from the IWC estimates.

2.2. ASCOS case study

A detailed description of the conditions encountered during the ASCOS campaign is available in Tjernström et al. (2012). Our focus here is on a stratocumulus deck observed between 30-31 August, while *Oden* was drifting with a 3×6 km^2 ice-floe at approximately 87° N. During that time, relatively quiescent large-scale conditions prevailed, characterized by a high-pressure system and large-scale subsidence in the free troposphere and only weak frontal passages (Tjernström et al., 2012).

Our simulations are initialized with thermodynamic and cloud liquid profiles representing conditions observed on 31 August at 06 UTC (Fig. 1). These profiles display a cloud layer between 550 and 900 m above ground level (a.g.l), at temperatures between -7^{o}C and -10^{o}C, capped by a temperature and humidity inversion, of about 5^{o}C and 0.5 g kg^{-1}, respectively. A weak secondary temperature inversion is also observed at about 370 m a.g.l., indicating that the cloud is decoupled from the surface; this type of vertical structure, with a decoupled surface and cloud layer, dominated during the whole ASCOS experiment (Sotiropoulou et al., 2014). More generally, this case study is representative of typical cloudy boundary layers over sea-ice, where co-existing temperature and humidity inversions are frequently observed (Sedlar et al., 2012), and clouds are often decoupled from any surface sources of e.g. moisture (Sotiropoulou et al., 2014).

The observed cloud layer remained ‘stable’ for about 12 hours prior to the selected profile and began dissipating after 31 August 9 UTC. A substantial reduction in the background aerosol concentration has been suggested as a possible cause for the sudden collapse of the cloud layer, which cannot be simulated by models without prognostic aerosol processes (Stevens et al., 2018). For this reason, we will use observational statistics from the period with the persistent stratocumulus conditions to evaluate our results, although simulations are allowed to run for 24 hours in a quasi-equilibrium state.

3. Model and Methods

3.1. LES set-up

The MIMICA LES (Savre et al., 2014) solves a set of non-hydrostatic prognostic equations for the conservation of momentum, ice-liquid potential temperature and total water mixing ratio with an anelastic approximation. A fourth order central finite-differences formulation determines momentum advection and a second order flux-limited version of the Lax-Wendroff scheme (Durran, 2010) is employed for scalar advection. Equations are integrated forward in time using a second order Leapfrog method and a modified Asselin filter (Williams, 2010). Subgrid scale turbulence is parameterized using the Smagorinsky-Lilly eddy-diffusivity closure (Lilly, 1992) and surface fluxes are calculated according to Monin-Obukhov similarity theory.

MIMICA employs a bulk microphysics scheme with a two-moment approach for cloud droplets, rain and cloud ice, graupel and snow particles. Mass mixing ratios and number concentrations are treated prognostically for these five hydrometeor classes, whereas their size distributions are defined by generalized Gamma functions. Cloud droplet and raindrop processes follow Seifert and Beheng (2001), while liquid/ice interactions are parameterized as in Wang and Chang (1993). Collisions between cloud ice larger than 150 μm and droplets larger than 15 μm, or raindrops, result in graupel formation; the efficiency of this conversion increases with increasing ice particle size. Graupel is also formed when snow and liquid particle collisions occur. These liquid particles can also be directly collected by graupel. Self-aggregation of cloud ice particles result in snow; this is the only snow formation mechanism in the default microphysics scheme. Self-aggregation is also allowed between snow particles, droplets larger than 15 μm and rain; aggregated snow particles and droplets are converted to graupels and raindrops, respectively. A simple parameterization for CCN activation is applied (Khvorostyanov and Curry, 2006), where the number of cloud droplets formed is a function of the modeled supersaturation and a prescribed background aerosol concentration. A detailed radiation solver (Fu and Liou, 1992) is coupled to MIMICA to account for cloud radiative properties when calculating the radiative fluxes.

The model configuration adopted is based on Ickes et al. (in prep.), who simulated the same case to examine the performance of various primary ice nucleation schemes. All simulations are performed on a 96×96×128 grid, with constant horizontal spacing dx = dy = 62.5 m. The simulated domain is 6×6 km^2 horizontally and 1.7 km vertically. At the surface and in the cloud layer the vertical grid spacing is 7.5 m, while between the surface and the cloud base it changes sinusoidally, reaching a maximum spacing of 25 m. The integration time step is variable (~ 1-3 sec), calculated continuously to satisfy the Courant-Friedrichs-Lewy criterion for the Leapfrog method. While this approach prevents numerical instabilities, its dynamic nature does not allow sensitivity simulations to be performed with exactly the same timestep. Lateral boundary conditions are periodic, while a sponge layer in the top 400 m of the domain dampens vertically-propagating gravity waves generated during the simulations. To accelerate the development of turbulent motions, the initial ice-liquid potential temperature profiles are randomly perturbed in the first 20 vertical grid levels with an amplitude less than 3×10^{-4} K.

Surface pressure and temperature are set to 1026.3 hPa and -3.2°C, respectively, constrained by surface sensors deployed on the ice-pack. The surface moisture is set to the saturation value, which reflects summer ice conditions. The surface albedo is assumed to be 0.85, which is representative of a multi-year ice pack. In MIMICA, subsidence is treated as a linear function of height: $w_{LS} = - D_{LS} \cdot z$, where D_{LS} is set 1.5×10^{-6} s^{-1} and z is the height in meters. Finally, the prescribed number of CCN is set to 30 cm^{-3} over the whole domain, which represents mean accumulation mode aerosol concentrations observed during the stratocumulus period (Igel et al., 2017). The duration of all simulations is 24 hours, where the first 4 hours constitute the spin-up period.

3.2 Ice Formation Processes in MIMICA

3.2.1 Primary ice production

Ickes et al. (in prep.) recently implemented several primary ice production (PIP) schemes in MIMICA. Here, we utilize the empirical ice nucleation active site density parameterization for immersion freezing, which is based on Connolly et al. (2009) and was further developed by Niemand et al. (2012) for Saharan dust particles. This formulation was used by Ickes et al. (2017) to describe the freezing behavior of different dust particle types, including microline (Appendix A). Microcline is a feldspar type that is known to be an efficient INP (Atkison et al., 2013). As no aerosol composition (or INP) measurements are available for the ASCOS campaign, we will use this INP type as a proxy for an aerosol constituent that can produce primary ice at the relatively warm sub-zero temperatures (-7°C to -10°C) of the initial observed cloud profile (Fig. 1a). At these temperatures it is reasonable to assume that most of the PIP occurs through immersion freezing (Andronache, 2017), i.e. that an aerosol must be both CCN active and contain ice-nucleating material to initiate ice production. Thus, we will simply assume that a specified fraction of the CCN population contains some efficient ice-nucleating material, here represented as feldspar, and match this fraction so that the model simulates reasonable values of LWP, IWP and ICNC (Appendix A, Text S1). Based on this procedure, we infer that the CCN population contains 5% microline, a value that results in realistic primary ICNCs (Wex et al., 2019), but in an underestimate of the IWP and an overestimate of the LWP (Text S1, Fig. S1). Note that even though we assume this relatively high fraction of ice-nucleating material (Text S1, Fig. S1), MIMICA still underestimates the IWP; we postulate that omitting the effects of secondary ice production may be the reason for this bias.

3.2.2 Ice multiplication from ice-ice collisions

The observed in-cloud temperatures are generally below the rime-splintering temperature range, except for the somewhat warmer temperatures near cloud base (Fig. 1a). Moreover, drop-shattering has been found ineffective for Arctic conditions (Fu et al., 2019; Sotiropoulou et al., 2020a). Our simulations further support the inefficiency of both these processes, as the concentration of large raindrops is too low (below 0.1 cm^{-3}) to initiate them (Fig. S1c). Hence we focus solely on ice multiplication from ice-ice collisions.

We implement the parameterization developed by Phillips et al. (2017a) in MIMICA and allow for ice multiplication from cloud ice-cloud ice, cloud ice-graupel, cloud ice-snow, snow-graupel, snow-snow and graupel-graupel collisions (Appendix B). The generated fragments are considered "small ice" crystals and are added to the cloud ice category in the model. The Phillips parameterization explicitly considers the effect of ice type, ice habit and rimed fractions of the colliding particles on fragment generation (Appendix B). The sensitivity of the model performance to these parameters is examined through sensitivity simulations. Additional tests are also performed to quantify the sensitivity to other sources of uncertainty, such as the applied correction for the sublimation effects in Vardiman's (1978) data (see section 1).

3.3 Sensitivity simulations

A detailed description of the sensitivity tests is provided in this section, while a summary is offered in Table 2.

3.3.1 The role of ice habit

Cloud ice observed within the examined temperature range can either be shaped as a dendrite or a plate, depending on the supersaturation with respect to ice (Pruppacher and Klett, 1997). However, as the mean vapor density excess in the simulated cloud layer varies between 0.03 and 0.22 g m^{-3}, it is not clear which shape should theoretically dominate (Pruppacher and Klett, 1997). Moreover, observations often indicate variable shapes within the same temperature conditions (Mioche et al., 2017). The formulation for ice multiplication due to break-up is substantially different for these two ice habits, with plates being included in the non-dendritic planar ice category (Appendix B).

MIMICA allows for variable treatment of the ice habit for the cloud ice category. These variations correspond to different characteristic parameters in the ($m = a_m D^{bm}$) and fallspeed-diameter ($v = a_v D^{bv}$) relationships (Table 2). To test the sensitivity of our results to the assumed cloud ice habit, the two simulations CNTRLDEN and CNTRLPLA are performed. 'CNTRL' refers to simulations that account only for PIP, while the suffixes 'DEN' and 'PLA' indicate dendritic and and non-dendritic planar cloud ice shape, respectively. Note that particle properties in CNTRLPLA simulations are adapted for plates (Pruppacher and Klett 1997), while the non-dendritic planar category in the Phillips parameterization encompasses a larger range of shapes (columns, needles, etc.).

Characteristic parameters for graupel in the default MIMICA version are relatively large, with a_v being one order of magnitude larger than the values adapted in other stratocumulus schemes (e.g. Morrison et al 2005). This difference has a weak impact on simulations that do not account for collisional break-up. However if break-up is active, fragment generation is a function of colliosional kinetic energy and the results become more sensitive to the choice of these parameters. Since Arctic clouds are characterized by weak convective motions and the formation of large rimed particles is not favored, the characteristic parameters of graupel are adjusted following Morrison et al. (2005) (Table 2).

3.3.2 The role of rimed fraction

F_{BR} is parameterized as a function of the rimed fraction (Ψ) of the ice crystal or snowflake that undergoes break-up; fragment generation from break-up of graupel does not depend on Ψ (see Appendix B). This parameter is not explicitly predicted in most bulk microphysics schemes, but can substantially affect the multiplication efficiency of the break-up process (Sotiropoulou et al., 2020a). For this reason, we will consider values of Ψ for cloud ice and snow between 0.1 (lightly rimed) and 0.4 (heavily rimed) (Phillips et al., 2017a, b); graupel particles are considered to have $\Psi \geq 0.5$. Both Sotiropoulou et al. (2020) and (2021) found that ice multiplication in polar clouds at temperatures above -8^{o}C is initiated only when a highly rimed fraction of cloud ice and snow is assumed. Their conclusions however may not be valid for our case, as the temperature and microphysical conditions are substantially different.

The effect of varying Ψ is examined for the two ice habits that prevail in the observed temperature range (Section 3.2.2). The performed simulations are referred to as BRDEN0.1, BRDEN0.2, BRDEN0.4, and BRPLA0.1, BRPLA0.2 BRPLA0.4, for dendrites and plates respectively (see Table 3). 'BR' indicates that collisional break-up is active, while the number 0.1-0.4 corresponds to the assumed value of Ψ. Note that assuming a constant rimed fraction for cloud ice and snow is unrealistic; this variable depends both on size and temperature. Yet the performed test will reveal whether a more realistic treatment of Ψ is essential for the description of collisional break-up. This information is useful particularly for implementations in climate models, where rimed fraction is not predicted and minimizing the computational cost of microphysical processes is important.

3.3.3 The impact of the ice hydrometeor type

The MIMICA LES has previously been used to study ice-ice collisions in Sotiropoulou et al. (2020), however, they used a parcel-model-based parameterization of the process, instead of implementing a break-up parameterization as a part of the MIMICA microphysics scheme. Sotiropoulou et al. argued that the efficiency of the process is likely underestimated in bulk microphysics schemes, where the dynamics of the ice particle spectrum is poorly represented and fixed particle properties are assumed typically for three ice types (cloud ice, graupel, snow), which is rather unrealistic. Their argument might be particularly true for the studied case where no snow is produced in the simulations with dendrites (Fig. S1d).

An interesting finding in Stevens et al. (2018), who compared the performance of several models that simulated the present case, was that the dominant ice particle type can be highly variable among the different models. For example, COSMO-LES and the Weather and Reseach Forecasting (WRF) model contain only a single ice particle category, which is cloud ice and snow respectively. MIMICA simulates both graupel and cloud ice, with former being substantially more abundant for the present case. COSMO-NWP (numerical weather prediction model) and UM-CASIM (the Met Office Unified Model with Cloud AeroSol Interacting Microphysics model) simulate snow and cloud ice. Cloud ice number concentrations were very limited in COSMO-NWP, while they were comparable to snow concentrations in UM-CASIM. These differences in ice particle properties result in very different ice water content (IWC) (see Fig. 11 in Stevens et al. (2018)) and can likely affect the efficiency of the break-up process. Nevertheless, MIMICA is the model that predicts more realistic IWC values in the study by Stevens et al. (2018), while most models (except UM-CASIM) predict very little ice content.

The main reason why MIMICA favors graupel formation is because all cloud ice particles with sizes larger than 150 μm that collide with droplets are added to this category. This is not the same in other schemes (e.g. Morrison et al., 2005) who considers that once cloud droplets are accreted on cloud ice, the rimed particle remains in the same ice category.

However adapting this approach in our model resulted in substantial enhancement of the cloud ice content and eventually to cloud glaciation (not showed). This indicates that different bulk microphysics schemes are tuned in very different ways. Another difference is that MIMICA allows for snow formation only through aggregation of cloud ice particles, while other microphysics schemes (Morrison et al., 2005; Morrison and Gettelman, 2008) also consider that cloud ice particles can grow to snowflakes through vapor deposition.

To test how differences in cloud ice content distribution among different hydrometeor types affect the multiplication efficiency of break-up, we further implemented a description for cloud ice-to-snow autoconversion (Appendix C) assuming that ice crystals with diameters larger than 500 μm are converted to snow. These simulations are referred to as: CNTRLDENauto, BRDEN0.2auto, BRDEN0.4auto for dendritic cloud ice/snow and CNTRLPLAauto, BRPLA0.2auto, BRPLA0.4auto when a non-dendritic planar ice habit is assumed. The number 0.2 or 0.4 indicates the prescribed rimed fraction. Tests with a lower separation diameter for cloud ice and snow showed little sensitivity to the choice of this parameter. In addition to the cloud ice-to-snow autoconversion description given in Appendix C, we also tested a different parameterization following Ferrier et al. (1994). In order to conserve the highest moments of the ice particle spectra, this parameterization assumes that the number of cloud ice are approximately constant by converting a few large ice crystals into snow. Yet, activating this process had very little impact on the macrophysical properties in simulations with inactive and active BR. While the results of this set of simulations are not shown, the reasons for a variable sensitivity to different descriptions of the autoconversion process are discussed in the text.

3.3.4 The impact of sublimation correction factor

As already discussed in section 1, the laboratory data used to develop the existing parameterization (Vardiman 1978; Takahashi et al. 1995) for break-up do not represent realistic in-cloud conditions. Phillips et al. (2017a) have attempted to quantify the impact of the simplifications in the laboratory set-ups. However, there is still significant uncertainty in the developed parameterization. For example, the correction factor induced in the fragility coefficient to account for the effects of sublimation on Vardiman's (1978) data was derived by the measurements of Takahashi et al. (1995) which were performed in near saturated conditions. This factor is thus highly uncertain and can substantially reduce the number of generated fragments (see Figs. 4-6 in Phillips et al. 2017a). To test the impact of this empirical correction, two simulations are perfomed in which this factor has been removed from the BR parameterization. These are referred as BRDENsub and BRPLAsub in the text (see Table 3). Finally, this modification is tested in conditions with enhanced snow formation, which are imposed by activating the cloud ice-to-snow autoconversion process (see section 3.3.3): these additional tests are referred as BRDENsubauto and BRPLAsubauto (Table 3). The rimed fraction in all these set-ups is set to 0.2.

4. Results

4.1 Sensitivity to ice habit and rimed fraction

The impact of the assumed ice habit and rimed fraction in the predicted liquid and ice water path (LWP, IWP) is presented in Fig. 2, while the median and interquartile statistics are summarized in Table 4. To quantify break-up efficiency, fragment generation rates (*PBR*) for the different collision types are shown in Fig. 3 (see Appendix B for detailed formulas). *PBR* results are only presented for cloud ice-graupel, graupel-snow and snow-snow collisions since we find negligible contributions from cloud ice-cloud ice, cloud ice-snow and graupel-graupel collisions.

Small differences are observed in the integrated cloud water quantities between CNTRLDEN and CNTRLPLA, as both produce median LWP values between 139-143 g m^{-2} and median IWP values of 1.8-2.2 g m^{-2}. Hence, both simulations overestimate cloud liquid (Fig. 2a-b) and underestimate ice compared to observations (Fig. 2c-d). Specifically, the median observed LWP (73.8 g m^{-2}) is overestimated by almost a factor of two, while IWP (7 g m^{-2}) is underestimated by about a factor of 3-3.5 (Table 4), which is larger than the uncertainty in the observations.

Activating break-up for dendrites results in improved simulated water properties: median LWP (IWP) decreases (increases) by 32-36 (2.2-3.8) g m^{-2}, with differences in the assumed rimed fraction having a weak impact on the results (Fig. 2a, c). The total fragment generation rates in Fig. 3 indicate that ice multiplication is dominated by snow-graupel collisions in these simulations. It is interesting that while snow is not formed in the CNTRLDEN simulation (Fig. S2), activation of break-up enhances cloud ice concentrations and thus the frequency of collisions between them, which promotes snow formation; break-up of snow eventually dominates the multiplication process (Fig. 3a,c,d). Generally, all total fragmentation rates in simulations with dendrites remain below 1.1 (L^{-1} s^{-1}), with small differences for different assumptions in Ψ (Fig. 3a,c,d).

Simulations with plates and a rimed fraction <= 0.2 produce similar macrophysical properties (Fig. 2b, d); LWP (IWP) decreases (increases) by 20-25 (2.4-2.6) g m^{-2}, suggesting lower efficiency of break-up compared to simulations with dendrites. This is also indicated by the lower fragment generation rates, which reach a maximum value of 0.8 (L^{-1} s^{-1}) at the end of BRPLA0.1 and BRPLA0.2 simulations (Fig. 3b,d,e). However, the cloud in BRPLA0.4 rapidly dissipates after 8 hours owing to excessive multiplication, with the total P_{BR} reaching a maximum of 12.8 $L^{-1}s^{-1}$ (Fig. 5b,d,f). Yet, a supercooled-liquid cloud reforms after 15 hours; LWP increases again to values larger than 100 g m^{-2} by the end of the simulated period (Fig. 2b), while IWP remains close to zero (Fig. 2d). Our findings are in agreement with Loewe et al. (2018) who showed that a prescribed ICNC value of 10 L^{-1} can lead to cloud dissipation for the specific case study.

Analysis of the simulation results indicates strong feedbacks between fragment generation, precipitation and evaporation/sublimation within the subcloud layer. To facilitate the discussion of these feedbacks, timeseries of mean surface precipitation rates and minimum sub-cloud saturation values are presented in Fig. 4, while the relative frequency distributions (RFD) of the charactrestic diameters of cloud ice and snow particles are shown in Fig. 5. Precipitation rates increase when break-up is activated (Fig. 4a-b), resulting in an overall lower total condensate. Moreover, saturation with respect to both liquid (Fig. 4c-d) and ice (Fig. 4e-f) decrease in all these simulations, except in BRPLA0.4, as increasing precipitation depletes the available water-vapor in the subcloud layer. This process further enhances the reduction of the total water path (LWP+IWP). An opposite behaviour is only found in BRPLA0.4 (Fig. 5d, f); the continuous multiplication shifts ice particle distributions to substantially smaller sizes (Fig. 5b, d), that can sublimate more efficiently in the sub-cloud layer. The feedbacks between break-up efficiency and changes in the simulated particle size distributions are discussed in more detail below.

Offline estimates of the cloud ice and snow diameters, calculated from the domain-averaged concentration profiles, are shown in Fig. 5. The RFDs of the cloud ice diameter exhibit a bimodal distribution for all simulations with dendrites (Fig. 5a). This is due to fact that cloud ice-to snow autoconversion is not treated in the default MIMICA model and ice crystals are allowed to grow to precipitation sizes without any size limits. Such precipitation-sized particles are represented by the second mode that corresponds to a size range similar to that for snow particles (Fig. 5c). The first mode of the cloud ice RFD does not play a significant role in the ice multiplication process due to the small sizes ~200-250 μm; this is proven by the fact that the characteristics of this mode do not change among the different simulations. On the contrary, with increasing rime fraction and thus increasing fragment generation, the second mode (that undergoes break-up) shifts to smaller sizes. While the assumption of a constant Ψ for this rather broad RFD is unrealistic, the fact that only a certain size range of cloud-ice undergoes break-up makes this simplification more reasonable. Also the comparable sizes of this cloud ice mode with snowflakes justify the adaption of the same Ψ for both ice types. Moreover, the increased fragment generation due to increasing Ψ is likely partly compensated by the the shift to smaller cloud ice and snow sizes, which are in turn expected to generate less fragments; this may explain the comparable fragmentation rates for all BRDEN set-ups (Fig. 3a,c,e).

The above conclusions also hold for simulations with plates and Ψ<=0.2. In BRPLA0.4 the fragment generation completely changes the RFD shape, resulting in a monomodal distribution with a substantially narrower range (Fig. 5b). Now all cloud particles can contribute to multiplication while they are not efficiently depleted by precipitation, resulting in an explosive ice production. Thus for such large changes in the shape of the RFD, the assumption of a constant Ψ throughout the simulation cannot be held and overestimations of this property can result in significant errors in cloud representation (Fig. 2b, d). While some atmospheric models explicitly predict rimed fraction (Morrison and Milbrandt 2015), such a detailed treatment is unlikely to be adapted in coupled General Circulation Models (GCMs) where minimizing computational costs is critical.

Generally, BR efficiency is found weak for the examined conditions, as ICNC enhancement rarely exceeds a factor of 2 in most simulations (Fig. 6a, b). This is substantially lower than the 10-20fold enhancement found in Sotiropoulou et al. (2020, 2021) for warmer mixed-phase clouds. However, note that an ICNC increase larger than a factor of 10, as in BRPLA0.4, would lead to cloud glaciation in the examined conditions (Fig. 6b). Yet this 1.5-2fold ICNC enhancement (Fig. 6a, b) is qualitatively consistent with in-situ Arctic cloud observations by Rangno and Hobbs (2001) who found that 35% of the observed ice particles where likely produced by fragmentation upon ice particle collisions. It is interesting that a weak ICNC increase can enhance IWP by a factor of ~5 and ~3.3 in simulations with dendrites (Fig. 6c) and plates (Fig. 6d), respectively; this enhancement becomes gradually weaker after twelve hours of simulation, stabilizing to a factor 2. This is likely due to a feedback between BR efficiency and ICNC concentrations; as ICNCs increase with time the size spectra is shifted to smaller sizes characterized by lower break-up efficiency. Overall, activation of break-up results in realistic IWP, while small improvements are found in the liquid properties; LWP remains above the observed interquartile range (Fig. 2a-b). Stevens et al. (2018) showed that simulations with interactive aerosols produce less LWP for the examined case, compared to simulations with a fixed background CCN concentration. Thus deviations between the simulated and observed LWP could be attributed to the simplified aerosol treatment, rather than to inadequacies in the representation of the break-up process.

4.2 Sensitivity to snow formation

Ice multiplication generally shifts cloud ice size distributions to smaller values. In simulations with moderate fragment generation, precipitation processes can balance continuous fragment generation due to break-up (Fig. 2). However, in BRPLA0.4 the larger fragment generation cannot be counterbalanced by precipitation, resulting in continuous accumulation of cloud ice particles within the cloud layer until the cloud glaciates. This is indicated by the lack of the bimodal shape in the RFD for BRPLA0.4 presented in Fig 5b. However, this behaviour can largely be supported by the fact that cloud-ice to snow autoconversion is not treated in the default MIMICA version, which can enhance snow formation and thus precipitation.

Activation of autoconversion in simulation set-ups that do not account for break-up has hardly any impact on IWP and LWP properties (Fig. 7). LWP and IWP statistics are similar between CNTRLPLA–CNTRPLAauto and CNTRLDEN–CNTRDENauto. The same holds for simulations with dendrites and active break-up. BRPLA0.2auto produces somewhat improved LWP (reduced by ~13 g m^{-2} compared to BRPLA0.2, Table 2), while the improvements are substantially larger in BRPLA0.4auto. The hypothesis that the implementation of cloud ice-to-snow autoconversion in the model can prevent the cloud glaciation occurring in BRPLA0.4 is confirmed in this simulation and the produced LWP and IWP statistics are similar to BRPLA0.2auto. However, this behaviour is not the same for all autoconversion schemes: application of the formulation described in Ferrier et al. (1994) does not prevent cloud dissipation (not shown). This is because Ferrier et al. (1994) assume that only very few large ice crystals are converted to snow and that the number concentration in the cloud ice category remains unaffected. To prevent explosive multiplication in this set-up, a reduction in cloud ice number concentration is essential.

Note that while with active break-up the model still does not reproduce liquid/ice partitioning correctly, there are significant improvements compared to the standard code. While CNTRLDENauto fails completely to reproduce the relationship between LWP and IWP (Fig. 8a, b), activation of break-up results in a partial agreement between modeled and observed LWP-IWP fields (Fig. 8a,c,d). Improvements of liquid-ice partitioning are also evident in BRPLA0.2auto and BRPLA0.4auto compared to CNTRLPLAauto (Fig. 9), with

BRPLA0.2auto being in better agreement with ASCOS observations. However, there are still significant deviations particularly in the representation of the liquid condensate which can be linked either to an underestimate in the ice production or to the simplified treatment of aerosols that act as CCN (Stevens et al. 2018).

4.3 Sensitivity to the sublimation correction factor

In section 4.1, simulations with plates were found more sensitive to increases in fragment generation induced by changes in the prescribed Ψ. In particular, ICNC enhancements of a factor of 10 resulted in cloud glaciation (Fig. 6b). Here we further examine the sensitivity of the results to increased ice multiplication by removing the correction factor for sublimation effects adapted in the Phillips et al (2017a) parameterization. For lightly rimed particles (Ψ=0.2), the reduction in fragment generation induced by this factor is largely variable depending on the collision type (see Figs 4b and 5a in Phillips et al 2017b).

Both BRDENsub and BRPLAsub simulations result in explosive ice multiplication and cloud dissipation (Fig. 10). In BRDENsub the cloud almost disappears after 6.5 hours and reforms after 8.5 hours (Fig 10a). In BRPLAsub the cloud glaciates within four hours and cloud-free conditions prevail for the rest of the simulation time (Fig 10b). Activation of cloud ice-to-snow autoconversion for this set-up prevents ice explosion and cloud dissipation in the simulation with dendrites but not with plates. In BRPLAsubauto, the autconversion process only delays cloud glaciation by 3 hours. The results indicate that while the determination of the correction factor is highly uncertain, its inclusion in the break-up parameterization is essential when applied to polar stratocumulus clouds, particularly in the case of non-dendritic planar ice. The high sensitivity that simulations exhibit to this parameter suggests that possible errors in the estimation of the correction factor can have a large impact on the multiplication effect predicted by Phillips et al. (2017) parameterization, particularly in conditions that favor the formation of non-dendritic planar ice.

5. Discussion

Ice formation processes in Arctic clouds are sources of great uncertainty in atmospheric models, often resulting in underestimation of the cloud ice content compared to observations. The poor representation of SIP has been suggested as the main cause behind this underestimation (Fridlind and Ackerman 2019), as rime-splintering is usually the only multiplication mechanism described in models. In-situ observations (Rangno and Hobbs, 1991;

Schwarzenboeck et al., 2009) and recent modeling studies (Sotiropoulou et al. 2020; 2021) suggest that collisional break-up is likely critical in polar mixed-phase clouds. However, due to the limited availability of laboratory studies and the unrealistic set-ups utilized in them (Vardiman 1978; Takahashi et al. 1995), the parameterization of this process is particularly challenging. Phillips et al. (2017a,b) have recently developed a physically-based numerical description for collisional break-up, constrained with existing laboratory data. This scheme estimates the number of fragments as a function of collisional kinetic energy, environmental temperature, size and rimed fraction of particle that undergoes break-up, while the influence of the different ice types and ice habits are also accounted.

While being more advanced than any other description for collisional break-up (e.g. Sullivan et al. 2018), the details of this parameterization cannot be addressed in most bulk microphysics schemes. While microphysics schemes with explicit prediction of the ice habit (e.g. Jensen et al 2017) or rimed fraction (e.g. Morrison and Milbradt 2015) have been developed, such detailed treatments are not utilized in coupled climate models as computational cost must be minimized. Thus the representation of break-up process in these models requires some simplifications. In this study we attempt to quantify the impact of ice multiplication through collisional break-up in summertime high-Arctic conditions and examine the sensitivity of the efficiency of this process to assumptions in the ice habit and rimed fraction of the colliding particles. We also examine how changes in ice type affect the multiplication process through activation of cloud-ice to snow autoconversion, a process not represented in the default model.

Simulations with a dendritic ice habit produce a realistic IWP when break-up is activated. The results show little sensitivity to assumptions in rimed fraction, suggesting that the lack of a prognostic treatment of this parameter in most bulk microphysics schemes is not detrimental for the description of the break-up process. Note that increases in Ψ result in increased ice multiplication that shifts the ice particle size distribution towards smaller values. These smaller particles can generate fewer fragments, which compensates for the enhancing effects of the larger Ψ. LWP is also somewhat improved compared to the simulation that does not account for SIP, however it still remains higher than the observed interquartile range.

Ice multiplication also improves the macrophysical state of the cloud in simulations with plates, as long as the cloud ice and snow particles that undergo break-up are assumed to be lightly rimed. These improvements are slightly smaller compared to the simulations with dendrites. However, prescribing a high rimed fraction for plates results in explosive multiplication, if cloud ice-to-snow autconversion is not accounted for in the model. This is because the larger fragment generation rates are not balanced by precipitation processes and the freshly formed small fragments accumulate in the cloud ice category, continuously feeding the multiplication process until the cloud glaciates.

Since fragment generation in the parameterization by Phillips et al. (2017a,b) is constrained based on unrealistic laboratory set-ups, there is considerable uncertainty in the estimated number of fragments. The impact of the correction for sublimation effects in Vardiman's (1978) data is examined by removing the relevant correction factor. This, however, resulted in cloud glaciation in both simulations with dendrites and plates, confirming that this correction is essential to avoid an unrealistic explosive multiplication. Enhanced precipitation through activation of cloud-ice to snow autoconversion can prevent cloud dissipation in all sensitivity tests that result in explosive multiplication, except for the set-up with non-dendritic planar ice that does not include the sublimation correction factor.

ICNC enhancement in the most realistic simulations rarely exceeds a factor of 2. Yano and Phillips (2011) developed a metric for multiplication efficiency $\hat{C} = 4c0atf\ tg$, where *c0* is the primary ice generation rate, *a* is the breakup rate (which is the product of the sweep-out rate and the number of fragments generated per collision), *tf a*nd *tg* are the timescale for fallout of large ice precipitation and time scale for conversion of small to large ice precipitation, respectively. Graupel formation occurs relatively fast in our model, thus our *tg* is smaller compared to the numbers adapted in previous studies (Yano and Phillips 2011; Phillips et al. 2017b; Sotiropoulou et al. 2020): 6.6 min and 7.5 min for BRPLA0.2 and BRDEN0.2 simulations, respectively. Also the number of fragments generated per snow-collision is found larger compared to warmer Arctic conditions: Sotiropoulou et al. (2020) found that maximum five fragments are generated per snow-graupel collision, while up to 13.7 (8.5) fragments are produced in the BRPLA0.2 (BRDEN0.2) simulations, respectively. While observations of Arctic clouds (Schwarzenboeck et al. 2009) also indicate that break-up of an ice particle usually produces less than 5 fragments, these estimates are only based on the examination of particles around 300 μm or roughly larger. In our simulations, mm-particles mainly contribute to ice multiplication (Fig. 5), suggesting that the estimated fragmentation number is not unreasonable. Neverthless, substituting these parameters in the above formula yields $\hat{C}$=1.6 and $\hat{C}$=2.2 for BRDEN0.2 and BRPLA0.2 simulations, which is 4.5-5.5 times lower than the estimated efficiency found in previous studies (Phillips et al. 2017b; Sotiropoulou et al. 2020) .

Sotiropoulou et al. (2020) found a 10-20 fold enhancement in ICNCs due to break-up compared to the available INPs and estimated $\hat{C}$=10 for Arctic clouds within the Hallet-Mossop temperature range. However their case is characterized by lower INP concentrations that do not exceed 0.1 L^{-1}, while in sensitivity tests of primary ice nucleation they showed that increasing INPs result in decreasing secondary ice production. In the present study, relatively high INP conditions are adapted. Primary ICNCs increase with time as the cloud cools through radiative cooling, reaching a maximum of 1 L^{-1} towards the end of the simulation. While primary ice formation in our set-up is likely overestimated (Fridlind et al., 2007; Wex et al., 2019), our results support the conclusions of Sotiropoulou et al. (2020) and further suggest that as primary ice nucleation becomes more and more enhanced at colder temperatures, ice multiplication from ice-ice collisions will likely become less significant. It is interesting that while laboratory experiments from Takahashi et al. (1995), based on collisions of two hailstones, suggest increasing ice multiplication with decreasing temperature from -3^{o}C to -15^{o}C, our findings indicate that this might not happen in the real atmosphere due to the increasing availability of INPs.

Finally, the possibility that ice multiplication is still underestimated in our simulations cannot be excluded, since MIMICA predicts that only 10-12% of the simulated ice particles in BRDEN0.2 and BRPLA0.2 simulations contribute to ice multiplication through break-up. Schwarzenboeck et al (2009) found indications of fragmentation in 55% of the examined ice particles, although natural fragmentation could only be confirmed for 18%, while their sample was characterized by relatively small sizes. Moreover, while processes like rime-splintering and drop-shattering are clearly ineffective in the examined conditions, the contribution from other SIP mechanisms has not been investigated, e.g. blowing snow and fragmentation of sublimating particles (Field et al. 2017). Sublimation of cloud ice particles can occur if cloud conditions become subsaturated with respect to ice; however a preliminary inspection of the domain-averaged supersaturation profiles did not reveal any such evidence. Furthermore, blowing snow is associated with relatively high wind speeds (Gossart et al, 2017), while during the examined ASCOS case the maximum wind speed never exceeded 5.2 m s^{-2} in the boundary layer.

6. Conclusions

In this study, ice multiplication from ice-ice collisions is implemented in the MIMICA LES, following Phillips et al. (2017a,b), to investigate the role of this process for ice-liquid partitioning in a summertime Arctic low-level cloud deck observed during ASCOS. The sensitivity of the simulated results to the prescribed ice habit and rimed fraction is examined. The impact of changes in ice content distribution among the three ice categories is also investigated by accounting for cloud ice-to-snow autoconversion and thus enhancing snow.

The last set of sensitivity tests concerns the sublimation correction factor adapted in the parameterization, which is a highly uncertain parameter. Our findings can be summarized as follows:

- For the simulated temperature range (-12.5 to -7 ^{o}C), ice multiplication from collisional break-up is generally weak, enhancing ICNCs by on average no more than a factor of 1.5-2 in the simulations that are most consistent with observations. Increases in ICNCs due to break-up are compensated by increased precipitation and sublimation in the sub-cloud layer. Simulation set-ups that produce a 10-fold ICNC enhancement result in cloud glaciation.
- While activation of break-up can substantially improve the agreement between modeled and observed cloud ice content, the impact on cloud liquid is weaker. Ice multiplication can decrease the median LWP by 25-35 g m^{-2}, resulting in better agreement with observations. Yet cloud liquid content remains overestimated in the model.
- Ice multiplication from break-up of dendrites is not very sensitive to assumptions regarding the rimed fraction. Break-up of lightly rimed non-dendritic planar ice also produces similar cloud water properties as in the simulations with dendrites. In contrast, break-up of highly rimed plates can lead to cloud glaciation, if cloud ice-to-snow autoconversion is not accounted for in the microphysics scheme. Activating cloud ice-to-snow autoconversion enhances the precipitation sink, which prevents accumulation of cloud ice particles, excessive multiplication and cloud glaciation.
- Removing the correction factor for sublimation effects from the Phillips et al. (2017a,b) parameterization results in cloud glaciation, independently of the assumed ice habit. Activation of cloud ice-to-snow autoconversion can prevent explosive multiplication in this set-up only for simulations with dendrites. The large sensitivity of the results suggest that this factor is likely the most important source of uncertainty in the representation of break-up, especially for non-dendritic planar ice particles.

The generally low sensitivity of our results to assumptions regarding ice habit and rimed fraction indicate that the lack of an explicit prediction of these properties in climate models is not detrimental for the representation of ice multiplication effects due to break-up in Arctic clouds. The sensitivity, however, is in some set-ups influenced by the way snow formation is treated, since snow precipitation can prevent continuous accumulation of ice particles within the cloud layer. Cloud ice-to-snow autoconversion appears to be a key process to sustain the balance between ice sources and sinks and this process is usually considered in most climate model bulk microphysics schemes (e.g. Murakami 1990; Morrison and Gettelman 2008). Finally, we acknowledge that the weak influence of the rimed fraction is likely limited for conditions characterized by weak break-up efficiency, as those examined here. Future model development plans include the treatment of rimed fraction as a prognostic variable; this is likely important for the study of collisional break-up effects in more convective clouds.

Code and data availability: ASCOS data are available at https://bolin.su.se/data/ascos/ . The modified LES code is available upon request.

Competing interests: The authors declare that they have no conflict of interest.

Author contribution: GS implemented the break-up parameterization in the LES, performed the simulations, analyzed the results and led manuscript writing. LI implemented the primary ice nucleation scheme. All authors contributed to the scientific interpretation, discussion and writing of the manuscript.

Acknowledgements: GS, AN and AE acknowledge support from the project IC-IRIM (project ID 2018-01760) funded by the Swedish Research Council for Sustainable Development (FORMAS) and the project FORCeS funded from Horizon H2020-EU.3.5.1. (project ID 821205). LI supported by Chalmers Gender Initiative for Excellence (Genie). The authors are also grateful to ASCOS scientific crew for the observational datasets used in this study and to two anonymous reviewers for very constructive comments. *The computations were enabled by resources provided by the Swedish National Infrastructure for Computing (SNIC) at the National Supercomputer Centre (NSC) partially funded by the Swedish Research Council through grant agreement no. 2016-07213.*

APPENDIX A: PRIMARY ICE PRODUCTION

The immersion freezing parameterization is based on the concept of ice nucleation active site density. The formulation of Niemand et al. (2012) is used, adapted for microline dust particles (Ickes et al., 2017). It is utilized here as the only primary ice production mechanism. In this scheme, the number of nucleated ice particles (N_{INP}, m^{-3}) is given as function of N_{CCN} and temperature T (^{o}C) :

$N_{INP} = XN_{CCN}\left(1 - e^{-4\pi r^2 n_s}\right)$,

where $n_s = e^{-aT+b}$. X is the percentage of N_{CCN} (m^{-3}) that acts as efficient INP, e.g. 50%, 10%, 5% (see Text S1 in Supporting Information) and n_s (m^{-2}) the ice nucleation active site density of the INP species assumed (here microcline). r =46.5·10^{-9} m is the mean radius of the accumulation aerosol mode measured during the examined ASCOS case (Ickes et al., in prep.). The temperature dependency is determined by the coefficients α=0.73°C^{-1} and b=9.63.

APPENDIX B: ICE MUTIPLICATION FROM ICE-ICE COLLISIONS

A bulk description of the collisional break-up process is applied, which is based on existing descpriptions of the interactions between the three ice particle types (cloud ice, snow and graupel) and within the same category (Wang and Chang 1993). Ice multiplication is allowed after cloud ice-cloud ice cloud ice-snow, cloud ice-graupel, graupel-snow, snow-snow and graupel-graupel collisions. For collisions between different ice types, the rate of number $(P_{n12} \wedge mass(P_{m12})$concentration of particle 1 that is collected by particle 2 is given:

$P_{n12} = \frac{\pi}{4}\rho E_{col} N_1 N_2$ (1)

$P_{q12} = \frac{\pi}{4}\rho E_{12} Q_1 N_2$ (2)

where subsrcript 'n' and 'm' denote number- and mass- weighted parameters, respectively. N and Q refer to number and mass concentration of the particle, while D and v represent its diameter and terminal velocity. a is the shape parameter of the size distribution for each particle, set to 2 for cloud ice (independently of the ice habit, 1 for snow and 0 for graupel, while b_v is a coefficient in the fallspeed-diameter relationship (see Section 3.3.1). E_{col} is the collection efficiency, given as a function of temperature (K): $E_{col=}$ $exp[0.09(T\text{-}273.15)]$. For self-collection, thus collisions between same ice types, the above equations take the form:

$P_{n11} = \frac{\pi}{2}\rho E_{col} N_1 N_1$ (3)

$P_{q11} = \frac{\pi}{2}\rho E_{col} N_1 Q_1$ (4).

The above equations are further used to determine collisions that result in ice multiplication, by replacing the collection efficiency with the term E^*=$1\text{-}E_{col}$. This means that the collisions that

Georgia 18/3/2021 13:54
Formatted: Highlight

do not result in aggregation are those that contribute to SIP. Since aggregation after cloud-ice-graupel and graupel-graupel collisions does not occur, we assume that 100% of these collisions result in multiplication: E^{*}=1.

The Phillips et al. (2017a) parameterization allows for varying treatment of F_{BR} depending on the ice crystal type and habit:

$$F_{BR} = \alpha A\left(1 - exp\left\{-\left[\frac{CK_o}{\alpha A}\right]^{\gamma}\right\}\right) \quad (5)$$

$K_o = \frac{m_1 m_2}{m_1 + m_2}\left(\Delta u_{n_{12}}\right)^2$ represents collisional kinetic energy and $\alpha = \pi D^2$, where D (in meters) is the size of the smaller ice particle which undergoes fracturing and α is its surface area. m_1, m_2 are the masses of the colliding particles and Δu_{n12} is the difference in their terminal velocities. A correction is further applied in Δu_{n12} to account for underestimates when $u_{n1} \approx u_{n2}$, following Mizuno et al. (1990) and Reisner et al. (1998):

$$\left|\Delta u_{n_{12}}\right| = ((1.7u_{n1} - u_{n2})^2 + 0.3u_{n1}u_{n2})^{1/2}$$

A represents the number density of the breakable asperities in the region of contact. C is the asperity-fragility coefficient, which is a function of a correction term (ψ) for the effects of sublimation based on the field observations by Vardiman (1978). Exponent γ is a function of rimed fraction for collisions that include cloud ice and snow. Particularly, for non-dendritic planar ice or snow, with rimed fraction $\Psi < 0.5$, that undergoes fracturing after collisions with other ice particles:

$$A = 1.58 \cdot 10^7(1 + 100\Psi^2)\left(1 + \frac{1.33 \cdot 10^{-4}}{D^{1.5}}\right) \quad (6),$$

$$C = 7.08 \times 10^6 \psi$$

$$\psi = 3.5 \times 10^{-3}$$

$$\gamma = 0.5 - 0.25\Psi$$

For fragmentation of dendrites, A and C are somewhat different :

$$A = 1.41 \cdot 10^6(1 + 100\Psi^2)\left(1 + \frac{3.98 \cdot 10^{-5}}{D^{1.5}}\right) \quad (7),$$

$$C = 3.09 \times 10^6 \psi$$

$$\psi = 3.5 \times 10^{-3}$$

$$\gamma = 0.5 - 0.25\Psi$$

For graupel-graupel collisions, an explicit temperature dependency is included in the equation,while γ is contant:

$A = \frac{a_o}{3} + \max\left(\frac{2a_o}{3} - \frac{a_o}{9}|T - 258|, 0\right)$ (8),

Aa_o=$3.78 \cdot 10^4 \cdot \left(1 + \frac{0.0079}{D^{1.5}}\right)$

$C = 6.3 \times 10^6$

$\psi = 3.5 \times 10^{-3}$

$\gamma = 0.3$

The parameterization was developed based on particles with diameters 500 μm < D < 5 mm, however Phillips et al. (2017a) suggest that it can be used for particle sizes outside the recommended range as long as the input variables to the scheme are set to the nearest limit of the range. Moreover, an upper limit for the number of fragments produced per collision is imposed, set to $F_{BR_{max}}$= 100 (Phillips et al., 2017a), for all collision types. The production rate of fragments is estimated using Eq. (1) or (3) and one of the proposed formulations for F_{BR} above, e.g. $P_{BR12}P_{n12}F_{BR}$. Whenever mass transfer also occurs, e.g. if assume that fragments ejected from snow-gruapel collisions are added to the cloud ice category, we assume that this is only 0.1% of colliding mass (Eq. (2) or (4)) that undergoes break-up (Phillips et al. 2017a).

APPENDIX C: CLOUD ICE - TO - SNOW AUTOCONVERSION

For cloud ice-to-snow autoconversion, we use the formula adapted in Wang and Chang (1993) for cloud ice-to-graupel and graupel-to-hail autoconversion:

$P_{q\mathrm{auto}} = Q_i e^{D_c\lambda}\left\{1 + D_c\lambda\left[1 + D_c\lambda\left(0.5 + \frac{D_c\lambda}{6}\right)\right]\right\}$

$P_{n\mathrm{auto}} = N_i e^{D_c\lambda}(1 + D_c\lambda)$

where $\lambda = \left[\frac{A_m\Gamma(\alpha+b_m+1)N_i}{\Gamma(\alpha+1)Q_i}\right]^{1/b_m}$

and D_c is the critical diameter that separates the two ice cateogries. N_i and Q_i are the number and mass cloud ice concentrations, respectively.

References

Andronache, C.: Characterization of Mixed-Phase Clouds: Contributions From the Field Campaigns and Ground Based Networks, in: Mixed-Phase Clouds: Observations and Modeling, edited by: Andronache, C., pp. 97–120, Elsevier, the Netherlands, UK, USA, https://doi.org/10.1016/B978-0-12-810549-8.00005-2, 2017.

Atkinson, J. D., Murray, B. J., Woodhouse, M. T., Whale, T. F., Baustian, K. J., Carslaw, K. S., Dobbie, S., O'Sullivan, D., and Malkin, T. L.: The importance of feldspar for ice nucleation by mineral dust in mixed-phase clouds, Nature, 498, 355–358, https://doi.org/10.1038/nature12278, 2013.

Bigg, E. K. and Leck, C.: Cloud-active particles over the central Arctic Ocean, J. Geophys. Res., 106, 32155–32166, doi:10.1029/1999JD901152, 2001.

Burt, M. A., Randall, D. A., and Branson, M. D.: Dark warming. Journal Climate, 29, 705–719, 2015

Cao, Y., Liang, S., Chen, X., He, T., Wang, D., and Cheng, X.: Enhanced wintertime greenhouse effect reinforcing Arctic amplification and initial sea-ice melting. Scientific Reports, 7, 8462, 2017

Choularton, T.W., Griggs, D.J. , Humood, B.Y., and Latham, J. : Laboratory studies of riming, and its relation to ice splinter production. Quart. J. Roy. Meteor. Soc., 106, 367–374, doi:https://doi.org/10.1002/qj.49710644809., 1980

Connolly, P. J., Möhler, O., Field, P. R., Saathoff, H., Burgess, R., Choularton, T., and Gallagher, M.: Studies of heterogeneous freezing by three different desert dust samples, Atmos. Chem. Phys., 9, 2805–2824, https://doi.org/10.5194/acp-9-2805-2009, 2009.

Cronin, T. W., and Tziperman, E. : Low clouds suppress Arctic air formation and amplify high-latitude continental winter warming. Proceedings of the National Academy of Sciences, 112, 11,490– 11,495, 2015

Durran, D.R.: Numerical Methods for Fluid Dynamics, Texts Appl. Math., 2nd ed., Springer, Berlin-Heidelberg, Germany, 2010.

Field, P., Lawson, P., Brown, G., Lloyd, C., Westbrook, D., Moisseev, A., Miltenberger, A., Nenes, A., Blyth, A., Choularton, T., Connolly, P., Bühl, J., Crosier, J., Cui, Z., Dearden, C., DeMott, P., Flossmann, A., Heymsfield, A., Huang, Y., Kalesse, H., Kanji, Z., Korolev, A., Kirchgaessner, A., Lasher-Trapp, S., Leisner, T., McFarquhar, G., Phillips, V., Stith, J., and Sullivan, S.: Chapter 7: Secondary ice production - current state of the science and recommendations for the future, Meteor. Monogr., doi:10.1175/AMSMONOGRAPHS-D-16-0014.1, 2017.

Fridlind, A. M., Ackerman, A. S., McFarquhar, G., Zhang, G., Poellot, M. R., DeMott, P. J., Prenni, A. J., and Heymsfield, A. J.: Ice properties of single-layer stratocumulus during the Mixed-Phase Arctic Cloud Experiment: 2. Model results., J. Geophys. Res., 112, D24202, https://doi.org/10.1029/2007JD008646, 2007.

Fridlind, A.M., van Diedenhoven, B., Ackerman, A.S., Avramov, A., Mrowiec, A., Morrison, H., Zuidema, P., and Shupe M.D.: A FIRE-ACE/SHEBA Case Study of Mixed-Phase Arctic Boundary Layer Clouds: Entrainment Rate Limitations on Rapid Primary Ice Nucleation Processes. J. Atmos. Sci., 69, 365–389, https://doi.org/10.1175/JAS-D-11-052.1, 2012

Fridlind, A. M., and Ackerman, A.S. : Simulations of Arctic Mixed-Phase Boundary Layer Clouds: Advances in Understanding and Outstanding Questions, Mixed-Phase Clouds: Observations and Modeling, 153-183, doi:10.1016/B978-0-12-810549-8.00007-6, 2019

Fu, Q, and Liou K.N: On the Correlated k-Distribution Method for Radiative Transfer in Nonhomogeneous Atmospheres, J. Atmos., 49(22): 2139–2156, doi: 10.1007/s00382-016-3040-8, 1992

Fu, S., Deng, X., Shupe, M.D., and Huiwen X.: A modelling study of the continuous ice formation in an autumnal Arctic mixed-phase cloud case, Atmos. Res., 228, 77-85, https://doi.org/10.1016/j.atmosres.2019.05.021, 2019

Gayet, J.-F., Treffeisen, R., Helbig, A., Bareiss, J., Matsuki, A., Herber, A., and Schwarzenboeck, A.: On the onset of the ice phase in boundary layer Arctic clouds, J. Geophys. Res., 114, D19201, doi:10.1029/2008JD011348, 2009

Gossart, A., Souverijns, N., Gorodetskaya, I. V., Lhermitte, S., Lenaerts, J. T. M., Schween, J. H., Mangold, A., Laffineur, Q., and van Lipzig, N. P. M.: Blowing snow detection from ground-based ceilometers: application to East Antarctica, The Cryosphere, 11, 2755–2772, https://doi.org/10.5194/tc-11-2755-2017, 2017.

Hallett, J. and Mossop, S. C.: Production of secondary ice particles during the riming process, Nature, 249, 26–28, doi:10.1038/249026a0, 1974.

Hong, S., J. Dudhia, and S. Chen: A Revised Approach to Ice Microphysical Processes for the Bulk Parameterization of Clouds and Precipitation. *Mon. Wea. Rev.*, **132**, 103–120, https://doi.org/10.1175/1520-0493(2004)132<0103:ARATIM>2.0.CO;2, 2004

Jensen A. A., Harrigton J. Y., Morrison H. and J.A. Milbrandt: Prediciting Ice Shape Evolution in a Bulk Microphysics Model, J. Atmos. Sci., 74(6), 2081-2104, https://doi.org/10.1175/JAS-D-16-0350.1, 2017

Ickes, L., Welti, A., and Lohmann, U.: Classical nucleation theory of immersion freezing: sensitivity of contact angle schemes to thermodynamic and kinetic parameters, Atmos. Chem. Phys., 17, 1713–1739, https://doi.org/10.5194/acp-17-1713-2017, 2017.

Ickes, L. and Ekman, A. : What is triggering freezing in warm Arctic mixed-phase clouds? A modelling study with MIMICA LES. in preparation, 2021

Igel, A. L., Ekman, A. M. L., Leck, C., Savre, J., Tjernström, M., and Sedlar, J.: The free troposphere as a potential source of Arctic boundary layer aerosol particles. Geophys. Res. Let.s, 44, 7053–706, doi:10.1002/2017GL073808, 2017

Kay, J. E., L'Ecuyer, T., Chepfer, H., Loeb, N., Morrison, A., & Cesana, G: Recent advances in Arctic cloud and climate research. Current Climate Change Reports, 2, 159–169, 2016

Khvorostyanov, V.I., and Curry J.A: Terminal Velocities of Droplets and Crystals: Power Laws with Continuous Parameters over the Size Spectrum. *J. Atmos. Sci.,* 59,1872 1884, https://doi.org/10.1175/1520-0469(2002)059<1872:TVODAC>2.0.CO;2, 2002

Khvorostyanov, V. I., and Curry, J. A.: Aerosol size spectra and CCN activity spectra: Reconciling the lognormal, algebraic, and power laws, J. Geophys. Res., 111, D12202, doi:10.1029/2005JD006532, 2006

Korolev, A., McFarquhar, G., Field, P.R., Franklin, C., Lawson, P., Wang, Z., Williams, E., Abel, S.J., Axisa, D., Borrmann, S., Crosier, J., Fugal, J., Krämer, M., Lohmann, U., Schlenczek, O., Schnaiter, M., and Wendisch, M.: Mixed-Phase Clouds: Progress and Challenges. Meteorological Monographs, 58, 5.1–5.50, https://doi.org/10.1175/AMSMONOGRAPHS-D-17-0001.1, 2017

Lauber, A., Kiselev, A., Pander, T., Handmann, P., and Leisner, T.: Secondary ice formation during freezing of levitated droplets, J. Atmos. Sci., 75, 2815–2826, https://doi.org/10.1175/JAS-D-18-0052.1, 2018.

Leck, C., Norman, M., Bigg, E. K., and Hillamo, R.: Chemi- cal composition and sources of the high Arctic aerosol rele- vant for fog and cloud formation, J. Geophys. Res., 107, 4135, doi:10.1029/2001JD001463, 2002.

Lilly, D.K.: A proposed modification to the Germano subgrid-scale closure method, Phys. Fluids, 4: 633–635, doi:10.1063/1.858280, 1992.

Loewe, K., Ekman, A. M. L., Paukert, M., Sedlar, J., Tjernström, M., and Hoose, C.: Modelling micro- and macrophysical contributors to the dissipation of an Arctic mixed-phase cloud during the Arctic Summer Cloud Ocean Study (ASCOS), Atmos. Chem. Phys., 17, 6693–6704, https://doi.org/10.5194/acp-17-6693-2017, 2017.

Lloyd, G., Choularton, T. W., Bower, K. N., Crosier, J., Jones, H., Dorsey, J. R., Gallagher, M. W., Connolly, P., Kirchgaessner, A. C. R., and Lachlan-Cope, T.: Observations and comparisons of cloud microphysical properties in spring and summertime Arctic stratocumulus clouds during the ACCACIA campaign, Atmos. Chem. Phys., 15, 3719–3737, https://doi.org/10.5194/acp-15-3719-2015, 2015.

Moore, R. H., Bahreini, R., Brock, C. A., Froyd, K. D., Cozic, J., Holloway, J. S., Middlebrook, A. M., Murphy, D. M., and Nenes, A.: Hygroscopicity and composition of

Alaskan Arctic CCN during April 2008, Atmos. Chem. Phys., 11, 11807–11825, https://doi.org/10.5194/acp-11-11807-2011, 2011

Moran, K. P., Martner, B. E., Post, M. J., Kropfli, R. A., Welsh, D. C., and Widener, K. B.: An unattended cloud-profiling radar for use in climate research, B. Am. Meteorol. Soc., 79, 443–455, doi:10.1175/1520-0477(1998)079<0443:AUCPRF>2.0.CO;2, 1998.

Morrison, H. and A. Gettelman, 2008: A New Two-Moment Bulk Stratiform Cloud Microphysics Scheme in the Community Atmosphere Model, Version 3 (CAM3). Part I: Description and Numerical Tests. J. Climate, 21, 3642–3659, https://doi.org/10.1175/2008JCLI2105.1

Morrison, H. and J.A. Milbrandt: Parameterization of cloud microphysics based on the prediction of bulk ice particle properties. Part I: Scheme description and idealized tests. *J. Atmos. Sci.*, *72*, 287-311. doi:10.1175/JAS-D-14-0065.1, 2015

Mioche, G., Jourdan, O., Delanoë, J., Gourbeyre, C., Febvre, G., Dupuy, R., Monier, M., Szczap, F., Schwarzenboeck, A., and Gayet, J.-F.: Vertical distribution of microphysical properties of Arctic springtime low-level mixed-phase clouds over the Greenland and Norwegian seas, Atmos. Chem. Phys., 17, 12845–12869, https://doi.org/10.5194/acp-17-12845-2017, 2017.

Murakami, M.: Numerical modeling of dynamical and microphysical evolution of an isolated convective cloud: The 19 July 1981 CCOPE cloud. J. Meteor. Soc. Japan, 68, 107-128, 1990

Mizuno, H.: Parameterization if the accretion process between different precipitation elements. J. Meteor. Soc. Japan, 57, 273-281, 1990

Morrison, H., Curry, J.A., and Khvorostyanov, V.I.: A New Double-Moment Microphysics Parameterization for Application in Cloud and Climate Models. Part I: Description, Atmos. Sci., 62, 3683-3704 62, 2005

Niemand, M., O. Möhler, B. Vogel, H. Vogel, C. Hoose, P. Connolly, H. Klein, H. Bingemer, P. DeMott, J. Skrotzki, and Leisner, T.: A Particle-Surface-Area-Based Parameterization of

Immersion Freezing on Desert Dust Particles. J. Atmos. Sci., 69, 3077–3092, https://doi.org/10.1175/JAS-D-11-0249.1 , 2012

Phillips, V. T. J., Yano, J.-I., and Khain, A.: Ice multiplication by breakup in ice-ice collisions. Part I: Theoretical formulation, J. Atmos. Sci., 74, 1705–1719, https://doi.org/10.1175/JAS-D-16-0224.1, 2017a.

Phillips, V.T., Yano, , J.-I., Formenton, M., Ilotoviz, E., Kanawade, V., Kudzotsa, I., Sun, J., Bansemer, A., Detwiler, A.G., Khain, A., and Tessendorf, S.A.: Ice Multiplication by Breakup in Ice–Ice Collisions. Part II: Numerical Simulations. J. Atmos. Sci., 74, 2789–2811, https://doi.org/10.1175/JAS-D-16-0223.1, 2017b.

Phillips, V.T., S. Patade, J. Gutierrez, and A. Bansemer, A.: Secondary Ice Production by Fragmentation of Freezing Drops: Formulation and Theory. J. Atmos. Sci., 75, 3031–3070, https://doi.org/10.1175/JAS-D-17-0190.1, 2018

Pruppacher, H.R., and Klett, J.D. : Microphysics of Clouds and Precipitation. 2nd Edition, Kluwer Academic, Dordrecht, 954 p., 1997

Rangno, A. L., and Hobbs, P. V.: Ice particles in stratiform clouds in the Arctic and possible mechanisms for the production of high ice concentrations, J. Geophys. Res., 106, 15,065–15,075, doi:10.1029/2000JD900286, 2001.

Reisner, J., Rasmussen, R. M., and Bruintjes, R. T.: Explicit forecasting of supercooled liquid water in winter storms using the MM5 mesoscale model, Quart. J. Roy. Meteor. Soc, 124(548), 1071{1107}, doi: 10.1002/qj.49712454804, 1998.

Roberts, G. C. and Nenes, A. A.: continuous-flow stream- wise thermal-gradient CCN chamber for atmospheric measurements, Aerosol Sci. Technol., 39, 206–221, doi:10.1080/027868290913988, 2005.

Savre, J, Ekman, AML, and Svensson, G.: Technical note: Introduction to MIMICA, a large-eddy simulation solver for cloudy planetary boundary layers, J. Adv. Model. Earth Syst., 6, doi:10.1002/2013MS000292, 2014.

Schwarzenboeck, A., Shcherbakov,V., Lefevre, R., Gayet, J.-F., Duroure, C., and Pointin, Y.: Evidence for stellar-crystal fragmentation in Arctic clouds,Atmos. Res.,92, 220–228, doi:10.1016/j.atmosres.2008.10.002, 2009

Sedlar, J., Shupe, M. D., and Tjernström, M.: On the relationship between thermodynamic structure, cloud top, and climate significance in the Arctic, J. Climate, 25, 2374–2393, doi:10.1175/JCLI-D-11-00186.1, 2012.

Seifert, A., and Beheng. K. D: A double-moment parameterization for simulating auto conversion, accretion and self collection, Atmos. Res., 59–60: 265–281, doi:10.1016/S0169-8095(01)00126-0, 2001.

Shupe, M. D., Uttal, T., and Matrosov, S. Y.: Arctic cloud micro- physics retrievals from surface-based remote sensors at SHEBA, J. Appl. Meteor. Clim., 44, 1544–1562, doi:10.1175/JAM2297.1, 2005.

Sotiropoulou, G, Sedlar, J, Tjernström, M, Shupe, MD, Brooks, IM, Persson, POG:The thermodynamic structure of summer Arctic stratocumulus and the dynamic coupling to the surface. Atmos. Chem. Phys., 14, 12573 – 12592, doi: 10.5194/acp-14-12573-2014, 2014.

Sotiropoulou, G., Sullivan, S., Savre, J., Lloyd, G., Lachlan-Cope, T., Ekman, A. M. L., and Nenes, A.: The impact of Secondary Ice Production on Arctic Stratocumulus, Atmos. Chem. Phys., 20, 1301–1316, https://doi.org/10.5194/acp-2019-804, 2020a.

Sotiropoulou G., Vignon E., Young G., Morrison H., O'Shea S.J., Lachlan-Cope T., Berne A., Nenes A.: Secondary ice production in Antarctic mixed-phase clouds: an underappreciated process in atmospheric models, Atmos. Chem. Phys. Discuss., https://doi.org/10.5194/acp-2020-328, in review, 2020b.

Stevens, R. G., Loewe, K., Dearden, C., Dimitrelos, A., Possner, A., Eirund, G. K., Raatikainen, T., Hill, A. A., Shipway, B. J., Wilkinson, J., Romakkaniemi, S., Tonttila, J., Laaksonen, A., Korhonen, H., Connolly, P., Lohmann, U., Hoose, C., Ekman, A. M. L., Carslaw, K. S., and Field, P. R.: A model intercomparison of CCN-limited tenuous clouds in the high Arctic, Atmos. Chem. Phys., 18, 11041–11071, https://doi.org/10.5194/acp-18-11041-2018, 2018.

Stocker, T.F., D. Qin, G.-K. Plattner, L.V. Alexander, S.K. Allen, N.L. Bindoff, F.-M. Bréon, J.A. Church, U. Cubasch, S. Emori, P. Forster, P. Friedlingstein, N. Gillett, J.M. Gregory, D.L. Hartmann, E. Jansen, B. Kirtman, R. Knutti, K. Krishna Kumar, P. Lemke, J. Marotzke, V. Masson-Delmotte, G.A. Meehl, I.I. Mokhov, S. Piao, V. Ramaswamy, D. Randall, M. Rhein, M. Rojas, C. Sabine, D. Shindell, L.D. Talley, D.G. Vaughan, and S.-P. Xie: Technical summary. In Climate Change 2013: The Physical Science Basis. Contribution of Working Group I to the Fifth Assessment Report of the Intergovernmental Panel on Climate Change. T.F. Stocker, D. Qin, G.-K. Plattner, M. Tignor, S.K. Allen, J. Doschung, A. Nauels, Y. Xia, V. Bex, and P.M. Midgley, Eds. Cambridge University Press, pp. 33-115, doi:10.1017/CBO9781107415324.005, 2013

Takahashi, T., Nagao, Y., and Kushiyama, Y.: Possible high ice particle production during graupel-graupel collisions, J. Atmos. Sci., 52, 4523–4527, doi:10.1175/1520-0469, 1995.

Tan, I., and Storelvmo, T. : Evidence of strong contributions from mixed-phase clouds to Arctic climate change. Geophysical Research Letters, 46, 2894-2902. https://doi.org/10.1029/2018GL081871, 2019

Taylor, P. C., Boeke, R. C., Li, Y., and Thompson, D. W. J.: Arctic cloud annual cycle biases in climate models, Atmos. Chem. Phys., 19, 8759–8782, https://doi.org/10.5194/acp-19-8759-2019, 2019.

Tjernström, M., Birch, C. E., Brooks, I. M., Shupe, M. D., Pers- son, P. O. G., Sedlar, J., Mauritsen, T., Leck, C., Paatero, J., Szczodrak, M., and Wheeler, C. R.: Meteorological conditions in the central Arctic summer during the Arctic Summer Cloud Ocean Study (ASCOS), Atmos. Chem. Phys., 12, 6863–6889, doi:10.5194/acp-12-6863-2012, 2012.

Tjernström, M., Leck, C., Birch, C. E., Bottenheim, J. W., Brooks, B. J., Brooks, I. M., Bäcklin, L., Chang, R. Y.-W., de Leeuw, G., Di Liberto, L., de la Rosa, S., Granath, E., Graus, M., Hansel, A., Heintzenberg, J., Held, A., Hind, A., Johnston, P., Knulst, J., Martin, M., Matrai, P. A., Mauritsen, T., Müller, M., Norris, S. J., Orellana, M. V., Orsini, D. A., Paatero, J., Persson, P. O. G., Gao, Q., Rauschenberg, C., Ristovski, Z., Sedlar, J., Shupe, M. D., Sierau, B., Sirevaag, A., Sjogren, S., Stetzer, O., Swietlicki, E., Szczodrak, M., Vaattovaara, P., Wahlberg, N., Westberg, M., and Wheeler, C. R.: The Arctic Summer Cloud Ocean Study

(AS- COS): overview and experimental design, Atmos. Chem. Phys., 14, 2823–2869, doi:10.5194/acp-14-2823-2014, 2014.

Vardiman, L.: The generation of secondary ice particles in clouds by crystal-crystal collision, J. Atmos. Sci., 35, 2168–2180, doi:10.1175/1520-0469, 1978.

Wang, C., and J. Chang, J.: A three-dimensional numerical model of cloud dynamics, microphysics, and chemistry. 1: Concepts and formulation, J. Geophys. Res., 98, 16,787–16,798, doi:10.1029/92JD01393, 1993.

Williams, P.D.: The RAW filter: An improvement to the Robert-Asselin filter in semi-implicit integrations, Mon. Weather Rev., 139: 1996–2007, doi:10.1175/2010 MWR3601.1, 2010

Yano, J.-I. and Phillips, V. T. J.: Ice-ice collisions: an ice multiplication process in atmospheric clouds, J. Atmos. Sci., 68, 322–333, doi:10.1175/2010JAS3607.1, 2011.

Yano, J.-I., Phillips, V. T. J., and Kanawade, V.: Explosive ice multiplication by mechanical break-up in-ice-ice collisions: a dynamical system-based study, Q. J. Roy. Meteor. Soc., 142, 867–879, https://doi.org/10.1002/qj.2687, 2015.

Young, G., Lachlan-Cope, T., O'Shea, S. J., Dearden, C., Listowski, C., Bower, K. N., Choularton T.W., and Gallagher M.W.: Radiative effects of secondary ice enhancement in coastal Antarctic clouds. Geophys. Res. Let. , 46 , 23122321, https://doi.org/10.1029/2018GL080551, 2019

Westwater, E. R., Han, Y., Shupe, M. D., and Matrosov, S. Y.: Analysis of integrated cloud liquid and precipitable water va- por retrievals from microwave radiometers during SHEBA, J. Geophys. Res., 106, 32019–32030, doi:10.1029/2000JD000055, 2001.

Wex, H., Huang, L., Zhang, W., Hung, H., Traversi, R., Becagli, S., Sheesley, R. J., Moffett, C. E., Barrett, T. E., Bossi, R., Skov, H., Hünerbein, A., Lubitz, J., Löffler, M., Linke, O., Hartmann, M., Herenz, P., and Stratmann, F.: Annual variability of ice-nucleating particle concentrations at different Arctic locations, Atmos. Chem. Phys., 19, 5293-5311, https://doi.org/10.5194/acp-19-5293-2019, 2019.

Tables:

Table 1: Characteristic parameters in the mass-diameter ($m = a_m D^{bm}$) and fallspeed-diameter ($v = a_v D^{bv}$) relationships (see Section 3.3.1).

Ice type	a_m	b_m	a_v	b_v
dendritic cloud ice	0.0233	2.29	5.02	0.48
planar cloud ice	1.43	2.79	17	0.62
snow	0.04	2	11.72	0.41
graupel	65	3	19.5	0.37

Table 2: List of sensitivity simulations (see Section 3.3).

Simulation	Breakup process	Ice Habit	Rimed Fraction	Other modifications
CNTRLDEN	off	dendrite	–	none
CNTRLPLA	off	plate	–	none
BRDEN0.1	on	dendrite	0.1	none
BRDEN0.2	on	dendrite	0.2	none
BRDEN0.4	on	dendrite	0.4	none
BRPLA0.1	on	plate	0.1	none
BRPLA0.2	on	plate	0.2	none
BRPLA0.4	on	plate	0.4	none
BRDEN0.4auto	on	dendrite	0.4	active cloud ice-to-snow autoconversion
BRPLA0.2auto	on	plate	0.2	active cloud ice-to-snow autoconversion
BRPLA0.4auto	on	plate	0.4	active cloud ice to snow autoconversion
BRDEN0.4auto	on	dendrite	0.4	active cloud ice-to-snow autoconversion
BRPLA0.2auto	on	plate	0.2	active cloud ice-to-snow autoconversion
BRDENsub	on	dendrite	0.2	no correction for sublimation effects
BRPLAsub	on	plate	0.2	no correction for sublimation effects
BRDENsubauto	on	dendrite	0.2	no correction for sublimation & cloud ice-to-snow autoconversion
BRPLAsubauto	on	plate	0.2	no correction for sublimation & cloud ice-to-snow autoconversion

Table 3: 25th, 50th (median) and 75th percentile of LWP and IWP timeseries. All variables are in g m^{-2}.

Simulation	25th perc. LWP	Median LWP	75th perc. LWP	25th perc. IWP	Median IWP	75th perc. IWP
ASCOS	52.7	73.8	89.3	4.2	7.0	11.4
CNTRLDEN	132.4	141.8	146.2	1.3	2.2	3.2
CNTRLPLA	130.9	139.1	145.7	1.2	1.8	2.7
BRDEN0.1	99.7	106.5	114.4	3.6	5.8	8.2
BRDEN0.2	107.4	109.1	118.0	4.4	6.0	7.2
BRDEN0.4	99.3	107.2	118.9	3.6	5.4	7.7
BRPLA0.1	110.0	116.6	128.8	2.4	4.2	6.9
BRPLA0.2	110.0	119.6	128.9	2.4	4.8	6.5
BRPLA0.4	0.76	39.7	99.3	0.0	0.0	1.6
CNTRDENauto	127.7	139.5	147.3	1.3	2.2	4.0
BRDEN0.2auto	100.9	109.1	116.1	3.9	5.8	7.1
BRDEN0.4auto	98.3	103.6	111.1	3.7	5.4	8.0
CNTRLPLAauto	129.3	139.8	146.1	1.5	2.2	4.3
BRPLA0.2auto	100.1	106.5	124.5	3.1	4.4	6.2
BRPLA0.4auto	104.0	110.0	117.1	1.9	4.5	6.5
BRDENsub	61.1	111.1	130.6	0.1	0.7	6.8
BRPLAsub	0.0	0.1	0.3	0.0	0.0	0.0
BRDENsubauto	98.8	102.5	113.9	2.9	5.0	7.5
BRPLAsubauto	0.2	22.5	94.6	0.0	0.1	0.5

Figures:

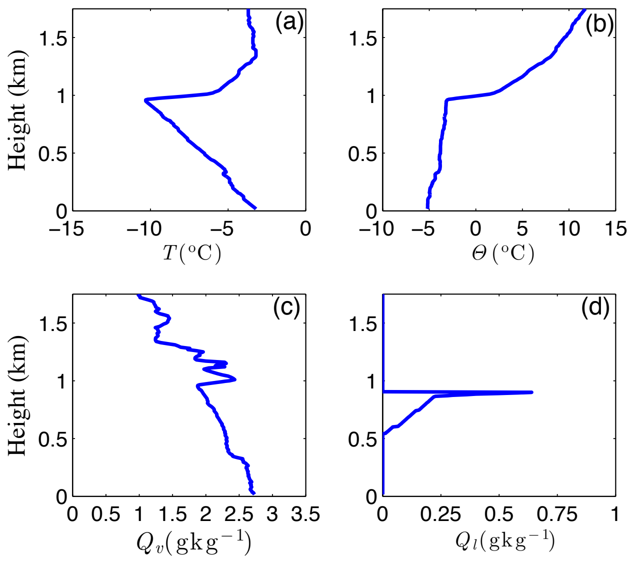

Figure 1: Radiosonde profiles of (a) temperature (T), (b) potential temperature (Θ), and (c) specific humitidy (Q_v) used to initialize the LES. The profile of cloud liquid (Q_l) in panel (d) is integrated from radiometer measurements.

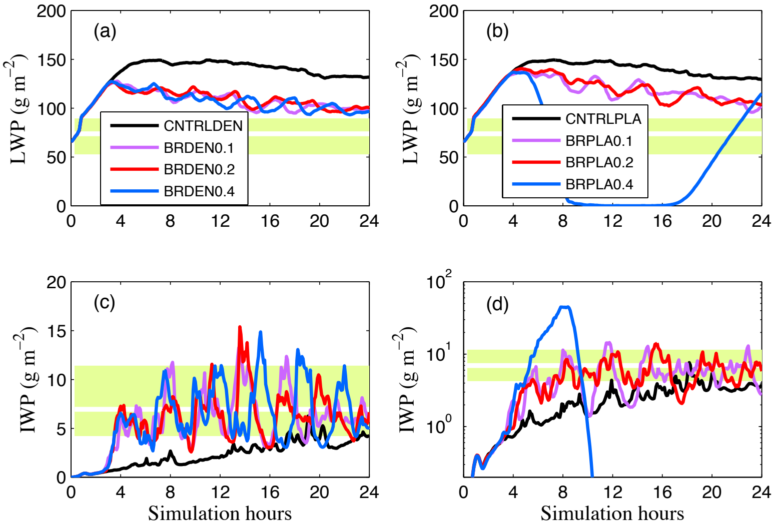

Figure 2: Timeseries of (a, b) LWP and (c, d) IWP for simulations with (a, c) dendrites and (b, d) plates. Light green shaded area indicates the interquartile range of observations, while the horizontal white line shows median observed values. Black lines represent simulations that account only for PIP. Purple, red and blue lines represent simulations with active break-up and a prescribed rimed fraction of 0.1, 0.2 and 0.4, respectively, for the cloud ice/snowflakes that undergo break-up. Note the logarithmic y-scale in panel (d).

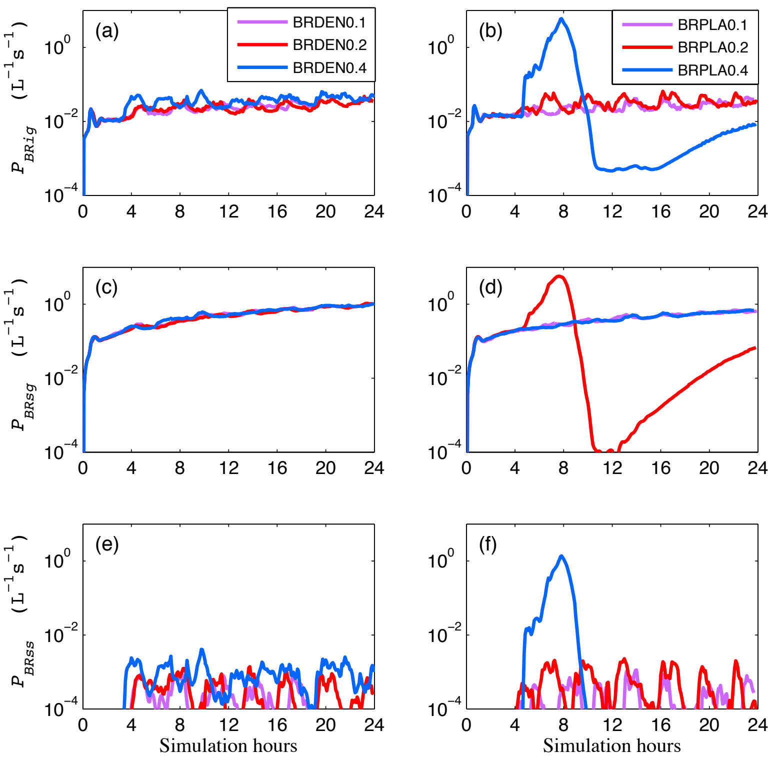

Figure 3: Timeseries of domain-averaged fragment generation rate ($L^{-1}s^{-1}$) from (a, b) cloud ice-graupel (P_{BRig}), (c, d) snow-graupel (P_{BRsg}) and (e, f) snow-snow (P_{BRss}) collisions, for simulations with varying rimed fractions for cloud ice/snow: 0.1 (purple), 0.2 (magenta), 0.4 (blue). Panels (a, c, e) correspond to simulations with dendrites, while (b, d, f) with plates. Note the logarithmic y-scale.

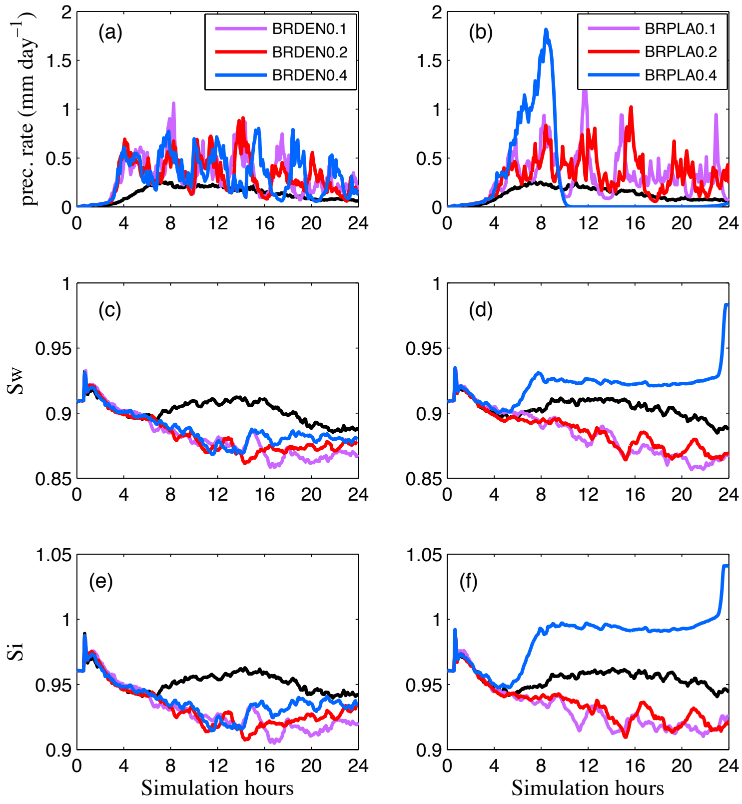

Figure 4: Timeseries of domain-averaged (a, b) surface precipitation rate (mm day^{-1}) and sub-cloud minimum saturation with respect to (c, d) water and (e, f) ice. Black line corresponds to simulation without active break-up. In the rest of the simulations, rimed fraction is set to 0.1 (purple), 0.2 (magenta) and 0.4 (blue). Panels (a, c, e) correspond to simulations with dendrites, while (b, d, f) with plates.

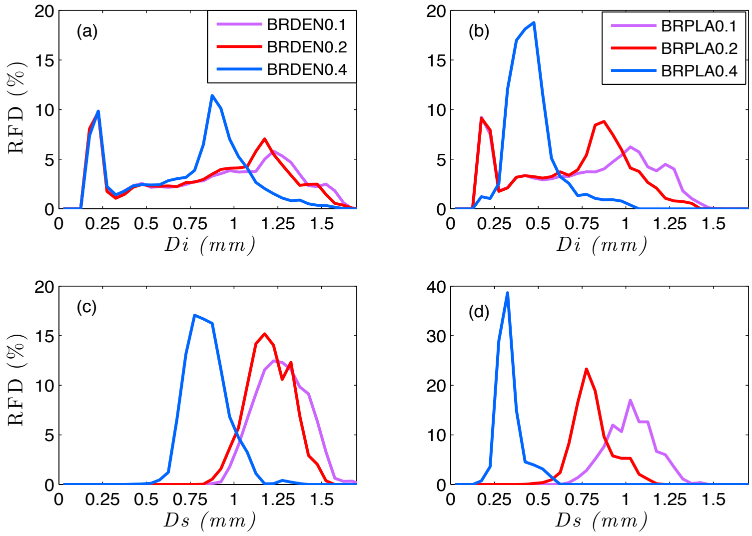

Figure 5 : Relative Frequency Distribution (RFD) of the mean (a, b) cloud ice and (c, d) snow diameter for simulations with (a, c) dendrites and (b, d) plates. Purple, red and blue lines correspond to a prescribed rimed fraction of 0.1, 0.2 and 0.4 for the cloud ice and snow particles than undergo break-up. Calculations are performed offline based on the domain-averaged cloud ice and snow concentrations.

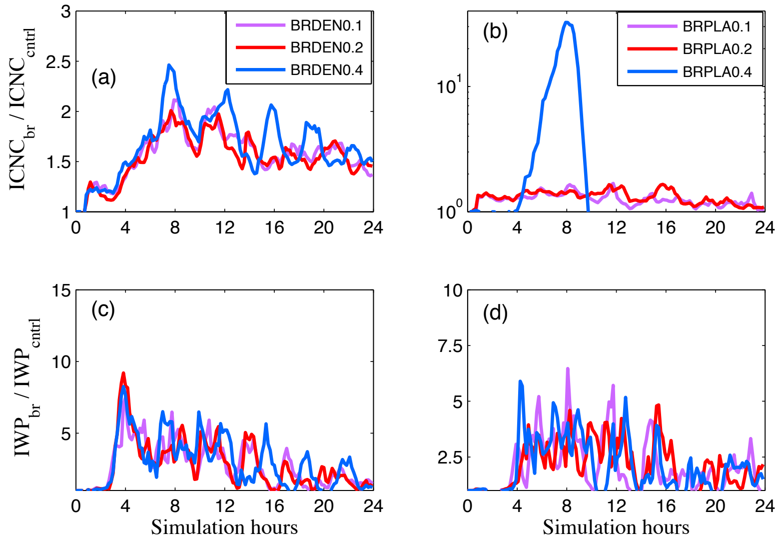

Figure 6: Timeseries of domain-averaged (a, b) ICNC and (c, d) IWP enhancement due to break-up. ICNC (IWP) enhancement is calculated by dividing the total ICNCs produced in each simulation with active ice multiplication with those produced by the control experiment that accounts only for PIP. The rimed fraction of cloud ice/snowflakes that undergo break-up is set to 0.1 (purple), 0.2 (magenta) and 0.4 (blue). Panels (a, c) correspond to simulations with dendrites, while (b, d) with plates.

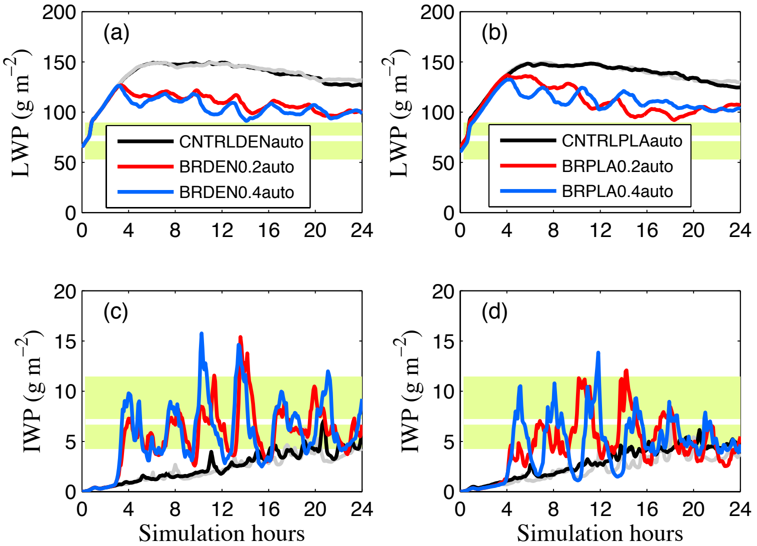

Figure 7: Same as Figure 2 but for simulations with active cloud ice-to-snow autoconversion. The cloud ice habit is set to (a, c) dendrites and (b, d) plates. Black lines represent simulations that account only for PIP. Red lines include the break-up process with a prescribed rimed fraction for cloud ice/snow set to 0.2. Blue lines are similar to red but with the prescribed fraction set to 0.4. Light grey lines represent baseline simulations that do not account for autoconversion: (a, c) CNTRLDEN and (b, d) CNTRLPLA (see Table 3).

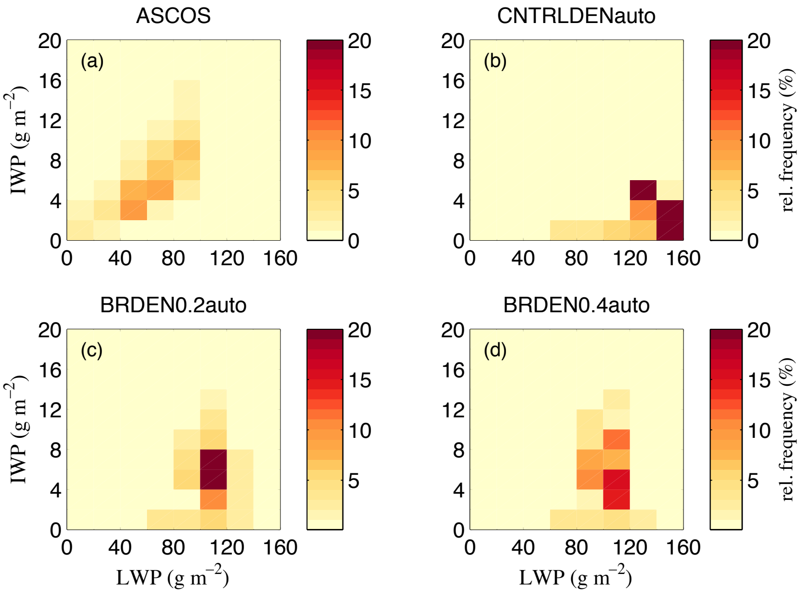

Figure 8: Relative frequency distribution of IWP (g m^{-2}) as a function of LWP (g m^{-2}) for (a) ASCOS, (b) CNTRLDENauto, (c) BRDEN0.2auto and (d) BRDEN0.4auto (see Table 3). Cloud ice-to-snow autoconversion is active in all model simulations. Collisional break-up is included only in panels (c-d) with the cloud ice/snow rimed fraction set to (c) 0.2 and (d) 0.4. In all simulations a dendritic cloud ice habit is assumed.

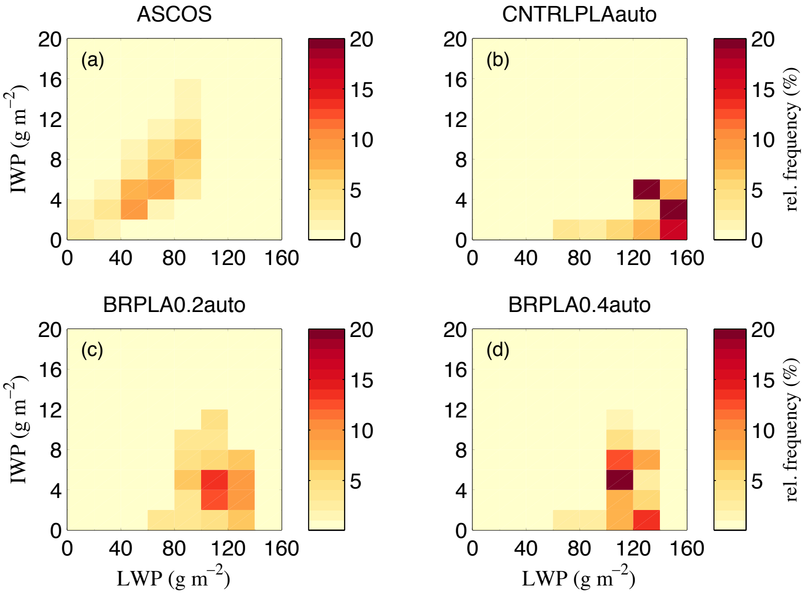

Figure 9: Relative frequency distribution of IWP (g m^{-2}) as a function of LWP (g m^{-2}) for (a) ASCOS, (b) CNTRLPLA, (c) BRPLA0.2auto and (d) BRPLA0.4auto (see Table 3). The set-up in each panel is similar to Fig. 8, except that in all simulations a planar cloud ice habit is assumed.

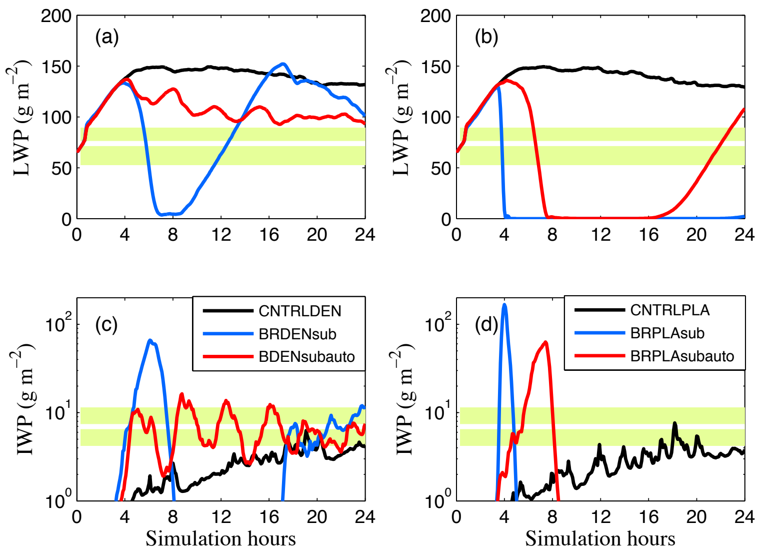

Figure 10: Similar to Fig. 2 but for simulations that do not include the sublimation correction factor in the break-up parameterization. Cloud-ice to snow autoconversion is active in BRDENsubauto and BRPLAsubauto simulations. Rimed fraction is set to 0.2.